**Table 1.** Frequency of lymph node (LN) metastasis by esophageal squamous cell carcinoma (ESCC) cell lines transplanted into nude mice

| | Cells | Left popliteal | Left inguinal | Paraaortic | Others | Total |
|---|---|---|---|---|---|---|
| Thoracic duct | SUm/c | 5/9 | 0/9 | 3/9 | 0/9 | 6/9 |
| | HSA/c | 8/9 | 0/9 | 1/9 | 0/9 | 8/9 |
| Primary tumor | KYSE510 | 1/10 | 0/10 | 0/10 | 0/10 | 1/10 |
| | KYSE770 | 0/9 | 0/9 | 0/9 | 0/9 | 0/9 |

Data represent mice/mice

| | LN metastasis (–) | LN metastasis (+) | Total |
|---|---|---|---|
| Cells from the thoracic duct | 4 | 14 | 18 |
| Cells from the primary tumor | 18 | 1 | 19 |
| Total | 22 | 15 | 37 |

$P < 0.0001$

Cell lines derived from thoracic duct lymph achieved a significantly higher rate of lymph node metastasis compared with cell lines from the primary tumor

pression was found to be associated with distant lymph node metastasis [88,104]. Thirty tumor cell lines showed overexpression of osteopontin protein compared with a normal esophageal epithelial cell line [88]. An inducible shRNA vector targeting osteopontin caused downregulation of osteopontin expression and decreased the motility, invasiveness, tumor-forming ability, and lymph node metastatic potential of highly metastatic tumor cells [88]. Furthermore, a high plasma OPN level was associated with lymph node metastasis, but not with the depth of tumor invasion [105].

Evidence has been obtained that an inverse correlation exists between the expression of the cysteine proteinase inhibitor stefin A and malignant progression [106]. Transfection of *stefin A* into an esophageal cancer cell line significantly reduced cathepsin B activity and inhibited the invasion of Matrigel. Overexpression of stefin A caused both in vitro and in vivo delay of growth and significantly inhibited lung metastasis. Transfection with *stefin A* caused a dramatic reduction of factor VIII staining in the xenograft tumors of mice [107]. Furthermore, cystatin B (one of the cysteine proteinase inhibitors that mainly inhibits cathepsin L) has been identified in ESCC, and reduced expression of cystatin B in esophageal carcinoma tissue is associated with lymph node metastasis [108]. Thus, cathepsins B and L may have a role in the metastasis of esophageal cancer.

The metastasis-associated protein MTA1 [109], PGP9.5/UCHL1 [110], elongation factor-1 (EF-1) delta [111], and fragile histidine triad (FHIT) genes [112] have also been reported to have a role in lymph node metastasis, but detailed analysis has not been done yet.

## Chromosomal changes

Chromosomal analysis has shown that loss of heterozygosity (LOH) on 13q is exclusively associated with lymph node metastasis and with a poor prognosis of esophageal squamous cell carcinoma [113]. Allelic loss of at least one marker is observed in 56.7% of tumors, and lymph node metastasis is significantly correlated with LOH. Loss at D13S260, D13S171, and D13S267 on 13q12-13 is frequently observed, and LOH at D13S171 shows a significant correlation with lymph node metastasis. Thus, allelic loss at 13q12-13 is closely associated with lymph node metastasis, suggesting that unidentified tumor suppressor gene(s) in this region might be involved [113]. Absence of gain of 8q24 and/or 20q12-qter has also been reported to be associated with freedom from lymph node metastasis in patients with superficial ESCC [114]. However, the actual genes affected at these loci have not been identified yet.

## Gene expression profile

### Stage-dependent gene expression

Sato et al. examined the expression of VEGF, MMP9, and E-cadherin in the early stage of lymph node metastasis (cancer cells occupying <50% of the lymph node) or the late stage (≥50% occupied) [115]. VEGF expression was downregulated in the late stage of lymph node metastasis whereas MMP-9 expression was elevated in the early stage. E-cadherin was expression is somewhat increased in the early stage but was suppressed again in the late stage of metastasis. In summary, the expression of VEGF, MMP-9, and E-cadherin changes during the process of lymph node metastasis by esophageal cancer, and the pattern of change is different for each molecule [115]. There is a complex network of genes involved in the process of tumor metastasis, and the role of each gene changes in importance at various points. Such changes of gene expression need to be observed and defined in more detail.

## Global gene expression profiling

Microarray technology allows us to assess the global gene expression profile of circulating tumor cells. Kan et al. examined the gene expression profile of 28 primary ESCCs with an 8000 cDNA microarray chip [116]. Lymph node metastasis-related genes were extracted with significance

analysis of microarrays (SAM) software, and an artificial neural network model was found to predict lymph node metastasis most accurately with 60 clones. The highest accuracy for predicting lymph node metastasis by this method was 77% (10/13) of new patients who were not used for gene selection by SAM analysis and 86% (24/28) overall (sensitivity, 15/17, 88%; specificity, 9/11, 82%) [116]. This system was also able to predict micrometastasis. Comparison of esophageal cancers with and without lymph node metastasis by SAM analysis did not detect any genes that have been reported to show a relationship to lymph node metastasis of esophageal cancer, such as extracellular matrix-degrading enzymes, cytoskeletal and adhesion proteins, or growth factors. However, some genes related to immunity, such as cytokines, and some apoptosis-related molecules were detected. This finding implies that the key factor involved in lymph node metastasis may be the interaction between invasive cancer cells and their microenvironment or host antitumor immunity [116].

Tamoto et al. identified 71 of 1289 cancer-related genes for which expression was correlated with the tumor stage [117]. In the case of lymph node metastasis, 44 genes showed predictive value. After training in classification with the selected features, tumor stage and lymph node metastasis were predicted in 18 cases used for validation with an accuracy of 94.4% and 88.9%, respectively [117].

Another study showed that 4155 genes were biologically significant in both ESCC and noncancerous esophageal tissue by Present Call analysis (hybridization by Affymetrix) [118]. A supervised learning method was used to select genes responsible for the development of ESCC. Intriguingly, there was no overlap between the 48 genes related to lymph node metastasis of pT1 tumors and the 30 genes related to lymph node metastasis of pT2-4 tumors, suggesting that ESCCs with different levels of invasiveness expressed different genes linked to lymph node metastasis. This result suggests that the depth of invasion must be considered when attempting to predict nodal metastasis of ESCC from the gene expression profile [118].

In an experimental study, the expression profile of 9206 genes in T.Tn-AT1 cells (a metastasizing cell line) and T. Tn cells (a nonmetastasizing cell line) was compared by cDNA microarray analysis [119], and only 34 genes showed a more than threefold difference in expression. Among these 34 genes, the expression of 8 genes (*KAL1, HPGD, NDN, REG1A, CXCR4, SPOCK, DIAPH2,* and *AIF1*) was downregulated, whereas the expression of 1 gene (*VNN2*) was upregulated in the metastasizing cells [119]. However, this result for CXCR4 is not consistent with recent clinical data [78].

These findings suggest that global gene expression profiling may be able to predict lymph node metastasis of ESCC, but the genes selected have differed among several studies, and further examination is needed to assess the clinical implications.

## Conclusion

A dynamic multistep process controls the establishment of metastasis of ESCC (Fig. 4, Table 2). Prediction of metastasis is the first step in selecting the optimum treatment. MMP inhibitors might be a possible treatment option, whereas the results of microarray analysis suggested that activation of immune surveillance may be another treatment strategy for esophageal cancer. Finally, shRNA decreased the metastasis of esophageal cancer in vitro, so molecular targeting could perhaps be employed to control metastasis of ESCC.

**Acknowledgments** This work was partly supported by a Grant-in-Aid from the Japanese Ministry of Education, Science and Culture (Grant 17390363).

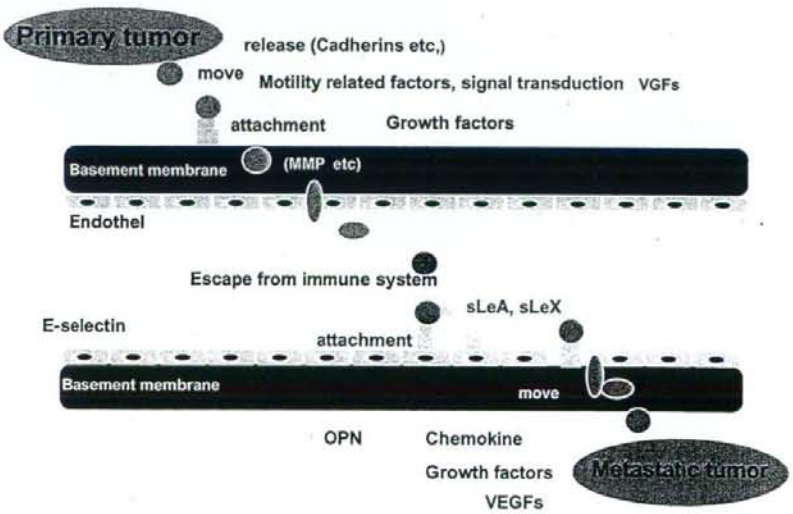


**Fig. 4.** Multistep genetic changes during the process of metastasis of ESCC

**Table 2.** Genes related to metastasis of ESCC

| Component | Function | Type of metastasis | References |
|---|---|---|---|
| **Adhesion molecule1** | | | |
| E-cadherin | Cell–cell adhesion | LN metastasis | 6, 7, 8, 10, 11, 12 |
| Alpha-catenin | Cell–cell adhesion | LN metastasis | 10 |
| Slug | Cell–cell adhesion | LN metastasis | 17 |
| TSLC1/IGSF4 | Cell–cell adhesion | LN metastasis | 19 |
| Thrombomodulin | Cell–cell adhesion, anticoagulant | LN metastasis | 21 |
| Desmoglein | Cell–cell adhesion | LN metastasis | 23 |
| FAK | Cellular focal adhesion | LN metastasis | 25 |
| **Attachment** | | | |
| SLex, sLea | Attachment between tumor and endothelial cells | Hematogenous metastasis | 92 |
| E-selectin | Attachment between tumor and endothelial cells | Hematogenous metastasis | 93 |
| **Matrix metalloproteinase** | | | |
| MMP | Degradation of extracellular matrix (ECM) | LN metastasis | 27, 28, 29, 30, 31, 32 |
| TIMP | Degradation of ECM | LN metastasis | 33, 34 |
| **Proliferation** | | | |
| Cyclin D1 | Regulation of cell cycle | Hematogenous metastasis | 37, 38, 39, 86 |
| p16/CDKN2 | Regulation of cell cycle | LN metastasis | 38, 86 |
| ODC Aurora | Biosynthesis of polyamins | LN metastasis | 42 |
| A/STK15/BTAK | Chromosomal distribution | LN metastasis | 45 |
| **Growth factor** | | | |
| EGFR | Cell growth | LN metastasis | 48 |
| TGF-alpha | Cell growth, angiogenesis | LN metastasis | 96 |
| VEGF-A | Neovascularization | LN metastasis | 95, 96 |
| VEGF-C | Lymph angiogenesis | LN metastasis | 98, 99, 101 |
| PD-ECGF, PynPase | Angiogenesis, 5-converting enzyme | LN metastasis | 96, 97 |
| HIF | Angiogenesis | LN metastasis | 101, 102 |
| NGF | Cell growth | LN metastasis | 51 |
| **Motility** | | | |
| Caveolin-1 | Plasma membrane, multifunction | LN metastasis | 67 |
| MRP1, KAI1 | Cell motility | LN metastasis | 75 |
| Fascin | Actin-binding protein | LN metastasis | 69 |
| AMF | Autocrine and motility | LN metastasis | 71 |
| Laminin-5-gamma-2 | Extracellular matrix protein | LN metastasis | 48 |
| **Chemokine** | | | |
| CCR7 | Chemotaxis | LN metastasis | 77 |
| CXCR4 | Chemotaxis | LN metastasis | 78, 119 |
| **Signal transduction** | | | |
| smad | Signal transduction | LN metastasis | 56 |
| Grb7 | Signal transduction | LN metastasis | 54 |
| RhoGTP | Signal transduction | LN metastasis | 60 |
| Activin-beta A | Signal transduction | LN metastasis | 58 |
| Shh, Gli | Signal transduction | LN metastasis | 65 |
| **Others** | | | |
| OPN | Multifunction | LN metastasis | 88, 104, 105 |
| Cathepsin B, L | Cyctein protease | LN metastasis | 107, 108 |
| 13q LOH | Unknown | LN metastasis | 113 |
| 8q24, 20q12-qter gain | Unknown | LN metastasis | 114 |

## References


1. Parkin DM, Pisani P, Ferlay J. Estimates of the worldwide incidence of 25 major cancer in 1990. Int J Cancer 1990;80:827–41.
2. Pisani P, Parkin DM, Bray F, Ferlay J. Estimates of the worldwide mortality from 25 cancers in 1990. Int J Cancer 1999;83:18–29.
3. Steeg PS. Tumor metastasis: mechanistic insights and clinical challenges. Nat Med 2006;12:895–904.
4. Bashyam MD. Understanding cancer metastasis. Cancer (Phila) 2002;94:1821–9.
5. Takeichi M. Cadherins: a molecular family important in selective cell-cell adhesion. Annu Rev Biochem 1990;59:237–52.
6. Doki Y, Shiozaki H, Tahara H, Inoue M, Oka H, Iihara K, et al. Correlation between E-cadherin expression and invasiveness in vitro in a human esophageal cancer cell line. Cancer Res 1993;53: 3421–6.
7. Shiozaki H, Kadowaki T, Doki Y, Inoue M, Tamura S, Oka H, et al. Effect of epidermal growth factor on cadherin-mediated adhesion in a human oesophageal cancer cell line. Br J Cancer 1995;71:250–8.
8. Tamura S, Shiozaki H, Miyata M, Kadowaki T, Inoue M, Matsui S, et al. Decreased E-cadherin expression is associated with haematogenous recurrence and poor prognosis in patients with squamous cell carcinoma of the oesophagus. Br J Surg 1996;83: 1608–14.
9. Nagafuchi A, Takeichi M, Tsukita S. The 102kd cadherin-associated protein: similarity to vinculin and posttranscriptional regulation of expression. Cell 1991;65:849–57.
10. Kadowaki T, Shiozaki H, Inoue M, Tamura S, Oka H, Doki Y, et al. E-cadherin and alpha-catenin expression in human esophageal cancer. Cancer Res 1994;54:291–6.
11. Research Committee on Malignancy of Esophageal Cancer, Japanese Society for Esophageal Diseases. Prognostic significance of cyclin D1 and E-cadherin in patients with esophageal squamous

cell carcinoma: multiinstitutional retrospective analysis. J Am Coll Surg 2001;192:708–18.
12. Shiozaki H, Doki Y, Yamana H, Isono K. A multi-institutional study of immunohistochemical investigation for the role of cyclin D1 and E-cadherin in superficial squamous cell carcinoma of the esophagus. J Surg Oncol 2002;79:166–73.
13. Cano A, Perez-Moreno MA, Rodrigo I, Locascio A, Blanco MJ, del Barrio MG, et al. The transcription factor snail controls epithelial-mesenchymal transitions by repressing E-cadherin expression. Nat Cell Biol 2000;2:76–83.
14. Batlle E, Sancho E, Franci C, Dominguez D, Monfar M, Baulida J, et al. The transcription factor snail is a repressor of E-cadherin gene expression in epithelial tumour cells. Nat Cell Biol 2000;2: 84–9.
15. Takeno S, Noguchi T, Fumoto S, Kimura Y, Shibata T, Kawahara K. E-cadherin expression in patients with esophageal squamous cell carcinoma: promoter hypermethylation, Snail overexpression, and clinicopathologic implications. Am J Clin Pathol 2004;12: 78–84.
16. Hajra KM, Chen DY, Fearon ER. The SLUG zinc-finger protein represses E-cadherin in breast cancer. Cancer Res 2002;62: 1613–8.
17. Uchikado Y, Natsugoe S, Okumura H, Setoyama T, Matsumoto M, Ishigami S, et al. Slug expression in the E-cadherin preserved tumors is related to prognosis in patients with esophageal squamous cell carcinoma. Clin Cancer Res 2005;11:1174–80.
18. Kuramochi M, Fukuhara H, Nobukuni T, Kanbe T, Maruyama T, Ghosh HP, et al. TSLC1 is a tumor-suppressor gene in human non-small-cell lung cancer. Nat Genet 2001;27:427–30.
19. Ito T, Shimada Y, Hashimoto Y, Kaganoi J, Kan T, Watanabe G, et al. Involvement of TSLC1 in progression of esophageal squamous cell carcinoma. Cancer Res 2003;63:6320–6.
20. Esmon CT. Protein C. Prog Hemost Thromb 1984;7:25–54.
21. Tezuka Y, Yonezawa S, Maruyama I, Matsushita Y, Shimizu T, Obama H, et al. Expression of thrombomodulin in esophageal squamous cell carcinoma and its relationship to lymph node metastasis. Cancer Res 1995;55:4196–200.
22. Pasdar M, Nelson WJ. Regulation of desmosome assembly in epithelial cells: kinetics of synthesis, transport, and stabilization of desmoglein I, a major protein of the membrane core domain. J Cell Biol 1989;109:163–77.
23. Natsugoe S, Aikou T, Shimada M, Kumanohoso T, Tezuka Y, Sagara M, et al. Expression of desmoglein 1 in squamous cell carcinoma of the esophagus. J Surg Oncol 1994;57:105–10.
24. Guan JL, Shalloway D. Regulation of focal adhesion-associated protein tyrosine kinase by both cellular adhesion and oncogenic transformation. Nature (Lond) 1992;358:690–2.
25. Miyazaki T, Kato H, Nakajima M, Sohda M, Fukai Y, Masuda N, et al. FAK overexpression is correlated with tumour invasiveness and lymph node metastasis in oesophageal squamous cell carcinoma. Br J Cancer 2003;89:140–5.
26. Khokha R, Denhardt DT. Matrix metalloproteinases and tissue inhibitor of metalloproteinases: a review of their role in tumorigenesis and tissue invasion. Invasion Metastasis 1989;9:391–405.
27. Shima I, Sasaguri Y, Kusukawa J, Yamana H, Fujita H, Kakegawa T, et al. Production of matrix metalloproteinase-2 and metalloproteinase-3 related to malignant behavior of esophageal carcinoma. A clinicopathologic study. Cancer (Phila) 1992;70:2747–53.
28. Yamashita K, Mori M, Shiraishi T, Shibuta K, Sugimachi K. Clinical significance of matrix metalloproteinase-7 expression in esophageal carcinoma. Clin Cancer Res 2000;6:1169–74.
29. Ding Y, Shimada Y, Gorrin-Rivas MJ, Itami A, Li Z, Hong T, et al. Clinicopathological significance of human macrophage metalloelastase expression in esophageal squamous cell carcinoma. Oncology 2002;63:378–84.
30. Etoh T, Inoue H, Yoshikawa Y, Barnard GF, Kitano S, Mori M. Increased expression of collagenase-3 (MMP-13) and MT1-MMP in oesophageal cancer is related to cancer aggressiveness. Gut 2000;47:50–6.
31. Yamashita K, Tanaka Y, Mimori K, Inoue H, Mori M. Differential expression of MMP and uPA systems and prognostic relevance of their expression in esophageal squamous cell carcinoma. Int J Cancer 2004;110:201–7.
32. Yamamoto H, Vinitketkumnuen A, Adachi Y, Taniguchi H, Hirata T, Miyamoto N, et al. Association of matrilysin-2 (MMP-26) expression with tumor progression and activation of MMP-9 in esophageal squamous cell carcinoma. Carcinogenesis (Oxf) 2004;25:2353–60.
33. Mori M, Mimori K, Sadanaga N, Inoue H, Tanaka Y, Mafune K, et al. Prognostic impact of tissue inhibitor of matrix metalloproteinase-1 in esophageal carcinoma. Int J Cancer 2000;88:575–8.
34. Miyazaki T, Kato H, Nakajima M, Faried A, Takita J, Sohda M, et al. An immunohistochemical study of TIMP-3 expression in oesophageal squamous cell carcinoma. Br J Cancer 2004;91: 1556–60.
35. Kanda Y, Nishiyama Y, Shimada Y, Imamura M, Nomura H, Hiai H, et al. Analysis of gene amplification and overexpression in human esophageal-carcinoma cell lines. Int J Cancer 1994;58: 291–7.
36. Nakagawa H, Zukerberg L, Togawa K, Meltzer SJ, Nishihara T, Rustgi AK. Human cyclin D1 oncogene and esophageal squamous cell carcinoma. Cancer (Phila) 1995;76:541–9.
37. Shinozaki H, Ozawa S, Ando N, Tsuruta H, Terada M, Ueda M, et al. Cyclin D1 amplification as a new predictive classification for squamous cell carcinoma of the esophagus, adding gene information. Clin Cancer Res 1996;2:1155–61.
38. Takeuchi H, Ozawa S, Ando N, Shih CH, Koyanagi K, Ueda M, et al. Altered p16/MTS1/CDKN2 and cyclin D1/PRAD-1 gene expression is associated with the prognosis of squamous cell carcinoma of the esophagus. Clin Cancer Res 1997;3:2229–36.
39. Shimada Y, Imamura M, Watanabe G, Uchida S, Harada H, Makino T, et al. Prognostic factors of oesophageal squamous cell carcinoma from the perspective of molecular biology. Br J Cancer 1999;80:1281–8.
40. Pegg AE. Regulation of ornithine decarboxylase. J Biol Chem 2006;28:14529–32.
41. Kubota S, Kiyosawa H, Nomura Y, Yamada T, Seyama Y. Ornithine decarboxylase overexpression in mouse 10T1/2 fibroblasts: cellular transformation and invasion. J Natl Cancer Inst 1997;89: 567–71.
42. Mafune K, Tanaka Y, Mimori K, Mori M, Takubo K, Makuuchi M. Increased expression of ornithine decarboxylase messenger RNA in human esophageal carcinoma. Clin Cancer Res 1999;5:4073–8.
43. Zhou H, Kuang J, Zhong L, Kuo WL, Gray JW, Sahin A, et al. Tumour amplified kinase STK15/BTAK induces centrosome amplification, aneuploidy and transformation. Nat Genet 1998;20: 189–93.
44. Sen S, Zhou H, Zhang RD, Yoon DS, Vakar-Lopez F, Ito S, et al. Amplification/overexpression of a mitotic kinase gene in human bladder cancer. J Natl Cancer Inst 2002;94(17):1320–9.
45. Tanaka E, Hashimoto Y, Ito T, Okumura T, Kan T, Watanabe G, et al. The clinical significance of Aurora-A/STK15/BTAK expression in human esophageal squamous cell carcinoma. Clin Cancer Res 2005;11:1827–34.
46. Ozawa S, Ueda M, Ando N, Shimizu N, Abe O. Prognostic significance of epidermal growth factor receptor in esophageal squamous cell carcinomas. Cancer (Phila) 1989;63:2169–73.
47. Yamamoto T, Kamata N, Kawano H, Shimizu S, Kuroki T, Toyoshima K, et al. High incidence of amplification of the epidermal growth factor receptor gene in human squamous carcinoma cell lines. Cancer Res 1986;46:414–6.
48. Fukai Y, Masuda N, Kato H, Fukuchi M, Miyazaki T, Nakajima M, et al. Correlation between laminin-5 gamma 2 chain and epidermal growth factor receptor expression in esophageal squamous cell carcinomas. Oncology 2005;69:71–80.
49. Dolle L, El Yazidi-Belkoura I, Adriaenssens E, Nurcombe V, Hondermarck H. Nerve growth factor overexpression and autocrine loop in breast cancer cells. Oncogene 2003;22:5592–601.
50. Davidson B, Reich R, Lazarovici P, Nesland JM, Skrede M, Risberg B, et al. Expression and activation of the nerve growth factor receptor TrkA in serous ovarian carcinoma. Clin Cancer Res 2003;9:2248–59.
51. Tsunoda S, Okumura T, Ito T, Mori Y, Soma T, Watanabe G, et al. Significance of nerve growth factor overexpression and its autocrine loop in oesophageal squamous cell carcinoma. Br J Cancer 2006;95:322–30.

52. Margolis B, Silvennoinen O, Comoglio F, Roonprapunt C, Skolnik E, Ullrich A, et al. High-efficiency expression/cloning of epidermal growth factor-receptor-binding proteins with Src homology 2 domains. Proc Natl Acad Sci U S A 1992;89:8894–8.
53. Manser J, Roonprapunt C, Margolis B. *C. elegans* cell migration gene mig-10 shares similarities with a family of SH2 domain proteins and acts cell nonautonomously in excretory canal development. Dev Biol 1997;184:150–64.
54. Tanaka S, Sugimachi K, Kawaguchi H, Saeki H, Ohno S, Wands JR. Grb7 signal transduction protein mediates metastatic progression of esophageal carcinoma. J Cell Physiol 2000;183:411–5.
55. Kretzschmar M, Massague J. SMADs: mediators and regulators of TGF-beta signaling. Curr Opin Genet Dev 1998;8:103–11.
56. Natsugoe S, Xiangming C, Matsumoto M, Okumura H, Nakashima S, Sakita H, et al. Smad4 and transforming growth factor beta1 expression in patients with squamous cell carcinoma of the esophagus. Clin Cancer Res 2002;8:1838–42.
57. Schuldiner M, Yanuka O, Itskovitz-Eldor J, Melton DA, Benvenisty N. Effects of eight growth factors on the differentiation of cells derived from human embryonic stem cells. Proc Natl Acad Sci U S A 2000;97:11307–12.
58. Yoshinaga K, Mimori K, Yamashita K, Utsunomiya T, Inoue H, Mori M. Clinical significance of the expression of activin A in esophageal carcinoma. Int J Oncol 2003;22:75–80.
59. Schmitz AA, Govek EE, Bottner B, Van Aelst L. Rho GTPases: signaling, migration, and invasion. Exp Cell Res. 2000;261:1–12.
60. Faried A, Faried LS, Kimura H, Nakajima M, Sohda M, Miyazaki T, et al. RhoA and RhoC proteins promote both cell proliferation and cell invasion of human oesophageal squamous cell carcinoma cell lines in vitro and in vivo. Eur J Cancer 2006;42:1455–65.
61. Ruiz i Altaba A, Palma V, Dahmane N. Gli and Hedgehog in cancer: tumors, embryos and stem cells. Nat Rev Neurosci 2002;3:24–33.
62. Magliano MP, Hebrok M. Hedgehog signaling in cancer formation and maintenance. Nat Rev Cancer 2003;3:903–11.
63. Berman DM, Karhadkar SS, Maltra A, Montes De Oca R, Gerstenblith MR, Briggs K, et al. Widespread requirement for Hedgehog ligand stimulation in growth of digestive tract tumours. Nature (Lond) 2003;425:846–51.
64. Karhadkar SS, Bova GS, Abdallah N, Dhara S, Gardner D, Maitra A, et al. Hedgehog signalling in prostate regeneration, neoplasia and metastasis. Nature (Lond) 2004;431:707–12.
65. Mori Y, Okumura T, Tsunoda S, Sakai Y, Shimada Y. The Gli-1 expression is associated with lymph node metastasis and tumor progression in esophageal squamous cell carcinoma. Oncology 2006;70:378–89.
66. Williams TM, Medina F, Badano I, Hazan RB, Hutchinson J, Muller WJ, et al. Caveolin-1 gene disruption promotes mammary tumorigenesis and dramatically enhances lung metastasis in vivo. Role of Cav-1 in cell invasiveness and matrix metalloproteinase (MMP-2/9) secretion. J Biol Chem 2004;279:51630–46.
67. Kato K, Hida Y, Miyamoto M, Hashida H, Shinohara T, Itoh T, et al. Overexpression of caveolin-1 in esophageal squamous cell carcinoma correlates with lymph node metastasis and pathologic stage. Cancer (Phila) 2002;94:929–33.
68. Hashimoto Y, Skacel M, Adams JC. Roles of fascin in human carcinoma motility and signaling: prospects for a novel biomarker? Int J Biochem Cell Biol 2005;37:1787–804.
69. Hashimoto Y, Ito T, Inoue H, Okumura T, Tanaka E, Tsunoda S, et al. Prognostic significance of fascin overexpression in human esophageal squamous cell carcinoma. Clin Cancer Res 2005;11:2597–605.
70. Nabi IR, Watanabe H, Raz A. Autocrine motility factor and its receptor: role in cell locomotion and metastasis. Cancer Metastasis Rev 1992;11:5–20.
71. Maruyama K, Watanabe H, Shiozaki H, Takayama T, Gofuku J, Yano H, et al. Expression of autocrine motility factor receptor in human esophageal squamous cell carcinoma. Int J Cancer 1995;64:316–21.
72. Patarroyo M, Tryggvason K, Virtanen I. Laminin isoforms in tumor invasion, angiogenesis and metastasis. Semin Cancer Biol 2002;12:197–207.
73. Ikeyama S, Koyama M, Yamaoko M, Sasada R, Miyake M. Suppression of cell motility and metastasis by transfection with human motility-related protein (MRP-1/CD9) DNA. J Exp Med 1993;177:1231–7.
74. Maecker HT, Todd SC, Levy S. The tetraspanin superfamily: molecular facilitators. FASEB J 1997;11:428–42.
75. Uchida S, Shimada Y, Watanabe G, Li ZG, Hong T, Miyake M, et al. Motility-related protein (MRP-1/CD9) and KAI1/CD82 expression inversely correlate with lymph node metastasis in oesophageal squamous cell carcinoma. Br J Cancer 1999;79:1168–73.
76. Muller A, Homey B, Soto H, Ge N, Catron D, Buchanan ME, et al. Involvement of chemokine receptors in breast cancer metastasis. Nature (Lond) 2001;410:50–6.
77. Ding Y, Shimada Y, Maeda M, Kawabe A, Kaganoi J, Komoto I, et al. Association of CC chemokine receptor 7 with lymph node metastasis of esophageal squamous cell carcinoma. Clin Cancer Res 2003;9:3406–12.
78. Kaifi JT, Yekebas EF, Schurr P, Obonyo D, Wachowiak R, Busch P, et al. Tumor-cell homing to lymph nodes and bone marrow and CXCR4 expression in esophageal cancer. J Natl Cancer Inst 2005;97:1840–7.
79. Izbicki JR, Hosch SB, Pichlmeier U, Rehders A, Busch C, Niendorf A, et al. Prognostic value of immunohistochemically identifiable tumor cells in lymph nodes of patients with completely resected esophageal cancer. N Engl J Med 1997;337:1188–94.
80. Sato F, Shimada Y, Li Z, Watanabe G, Maeda M, Imamura M. Lymph node micrometastasis and prognosis in patients with oesophageal squamous cell carcinoma. Br J Surg 2001;88:426–32.
81. Scheunemann P, Izbicki IR, Pantel K. Tumorigenic potential of apparently tumor-free lymph nodes. N Engl J Med 1999;340:1687.
82. Nagatani S, Shimada Y, Sato F, Watanabe G, Maeda M, Kaganoi J, et al. Expression of E-cadherin, cyclin D1, matrix metalloproteinase 9, and vascular endothelial growth factor in primary tumor of esophageal squamous cell carcinoma does not predict lymph node micrometastasis. Esophagus 2005;2:71–5.
83. Mori M, Mimori K, Ueo H, Tsuji K, Shiraishi T, Barnard GF, et al. Clinical significance of molecular detection of carcinoma cells in lymph nodes and peripheral blood by reverse transcription-polymerase chain reaction in patients with gastrointestinal or breast carcinomas. J Clin Oncol 1998;16:128–32.
84. Nakashima S, Natsugoe S, Matsumoto M, Miyazono F, Nakajo A, Uchikura K, et al. Clinical significance of circulating tumor cells in blood by molecular detection and tumor markers in esophageal cancer. Surgery (St. Louis) 2003;133:162–9.
85. Kaganoi J, Shimada Y, Kano M, Okumura T, Watanabe G, Imamura M. Detection of circulating oesophageal squamous cancer cells in peripheral blood and its impact on prognosis. Br J Surg 2004;91:1055–60.
86. Watanabe H, Tachimori Y, Katon H, Nakanishi K, Ochiai A, Gyotoku M, et al. Tumor progression of cancer cells derived from lymph fluid of thoracic duct for esophageal cancer patients by orthotopic transplantation on nude rat. Biotherapy 1996;10:1332–7.
87. Nakaji T, Kataoka TR, Watabe K, Nishiyama K, Nojima H, Shimada Y, et al. A new member of the GTPase superfamily that is upregulated in highly metastatic cells. Cancer Lett 1999;147:139–47.
88. Ito T, Hashimoto Y, Tanaka E, Kan T, Tsunoda S, Sato F, et al. An inducible short-hairpin RNA vector against osteopontin reduces metastatic potential of human esophageal squamous cell carcinoma in vitro and in vivo. Clin Cancer Res 2006;12:1308–16.
89. Haraguchi N, Utsunomiya T, Inoue H, Tanaka F, Mimori K, Barnard GF, et al. Characterization of a side population of cancer cells from human gastrointestinal system. Stem Cells 2006;24:506–13.
90. Ban S, Ishikawa K, Kawai S, Koyama-Saegusa K, Ishikawa A, Shimada Y, et al. Potential in a single cancer cell to produce heterogeneous morphology, radiosensitivity and gene expression. J Radiat Res (Tokyo) 2005;46:43–50.
91. Kannagi R. Carbohydrate-mediated cell adhesion involved in hematogenous metastasis of cancer. Glycoconj J 1997;14:577–84.
92. Makino T, Shimada Y, Maeda M, Komoto I, Imamura M. Carbohydrate antigens as a risk factor for hematogenous recurrence

of esophageal squamous cell carcinoma patients. Oncol Rep 2001;8:981–5.
93. Shimada Y, Maeda M, Watanabe G, Imamura M. High serum soluble E-selectin levels are associated with postoperative haematogenic recurrence in esophageal squamous cell carcinoma patients. Oncol Rep 2003;10:991–5.
94. Roy H, Bhardwaj S, Yla-Herttuala S. Biology of vascular endothelial growth factors. FEBS Lett 2006;580:2879–87.
95. Uchida S, Shimada Y, Watanabe G, Tanaka H, Shibagaki I, Miyahara T, et al. In oesophageal squamous cell carcinoma vascular endothelial growth factor is associated with p53 mutation, advanced stage and poor prognosis. Br J Cancer 1998;77:1704–9.
96. Li Z, Shimada Y, Uchida S, Maeda M, Kawabe A, Mori A,et al. TGF-alpha as well as VEGF, PD-ECGF and bFGF contribute to angiogenesis of esophageal squamous cell carcinoma. Int J Oncol 2000;17:453–60.
97. Yamagata M, Mori M, Mimori K, Mafune KI, Tanaka Y, Ueo H, et al. Expression of pyrimidine nucleoside phosphorylase mRNA plays an important role in the prognosis of patients with oesophageal cancer. Br J Cancer 1999;79:565–9.
98. Kitadai Y, Amioka T, Haruma K, Tanaka S, Yoshihara M, Sumii K, et al. Clinicopathological significance of vascular endothelial growth factor (VEGF)-C in human esophageal squamous cell carcinomas. Int J Cancer 2001;93:662–6.
99. Matsumoto M, Natsugoe S, Okumura H, Arima H, Yanagita S, Uchikado Y, et al. Overexpression of vascular endothelial growth factor-C correlates with lymph node micrometastasis in submucosal esophageal cancer. J Gastrointest Surg 2006;10:1016–22.
100. Pouyssegur J, Dayan F, Mazure NM. Hypoxia signaling in cancer and approaches to enforce tumour regression. Nature (Lond) 2006;441:437–43.
101. Katsuta M, Miyashita M, Makino H, Nomura T, Shinji S, Yamashita K, et al. Correlation of hypoxia inducible factor-1-alpha with lymphatic metastasis via vascular endothelial growth factor-C in human esophageal cancer. Exp Mol Pathol 2005;78: 123–30.
102. Kurokawa T, Miyamoto M, Kato K, Cho Y, Kawarada Y, Hida Y, et al. Overexpression of hypoxia-inducible-factor 1alpha (HIF-1alpha) in oesophageal squamous cell carcinoma correlates with lymph node metastasis and pathologic stage. Br J Cancer 2003;89: 1042–7.
103. Furger KA, Menon RK, Tuck AB, Bramwell VH, Chambers AF. The functional and clinical roles of osteopontin in cancer and metastasis. Curr Mol Med 2001;1:621–32.
104. Kita Y, Natsugoe S, Okumura H, Matsumoto M, Uchikado Y, Setoyama T, et al. Expression of osteopontin in oesophageal squamous cell carcinoma. Br J Cancer 2006;95:634–8.
105. Shimada Y, Watanabe G, Kawamura J, Soma T, Okabe M, Ito T, et al. Clinical significance of osteopontin in esophageal squamous cell carcinoma: comparison with common tumor markers. Oncology 2005;68:285–92.
106. Sloane BF, Moin K, Krepela E, Rozhin J. Cathepsin B and its endogenous inhibitors: the role in tumor malignancy. Cancer Metastasis Rev 1990;9:333–52.
107. Li W, Ding F, Zhang L, Liu Z, Wu Y, Luo A, et al. Overexpression of stefin A in human esophageal squamous cell carcinoma cells inhibits tumor cell growth, angiogenesis, invasion, and metastasis. Clin Cancer Res 2005;11:8753–62.
108. Shiraishi T, Mori M, Tanaka S, Sugimachi K, Akiyoshi T. Identification of cystatin B in human esophageal carcinoma using differential displays in which the gene expression is related to lymph-node metastasis. Int J Cancer 1998;79:175–8.
109. Toh Y, Kuwano H, Mori M, Nicolson GL, Sugimachi K. Overexpression of metastasis-associated MTA1 mRNA in invasive oesophageal carcinomas. Br J Cancer 1999;79:1723–6.
110. Mandelker DL, Yamashita K, Tokumaru Y, Mimori K, Howard DL, Tanaka Y, et al. PGP9.5 promoter methylation is an independent prognostic factor for esophageal squamous cell carcinoma. Cancer Res 2005;65:4963–8.
111. Ogawa K, Utsunomiya T, Mimori K, Tanaka Y, Tanaka F, Inoue H, et al. Clinical significance of elongation factor-1 delta mRNA expression in oesophageal carcinoma. Br J Cancer 2004;91:282–6.
112. Tzao C, Sun GH, Tung HJ, Hsu HS, Hsu WH, Wang YC, et al. Reduced acetylated histone H4 is associated with promoter methylation of the fragile histidine triad gene in resected esophageal squamous cell carcinoma. Ann Thorac Surg 2006;82:396–401.
113. Harada H, Tanaka H, Shimada Y, Shinoda M, Imamura M, Ishizaki K. Lymph node metastasis is associated with allelic loss on chromosome 13q12-13 in esophageal squamous cell carcinoma. Cancer Res 1999;59:3724–9.
114. Ueno T, Tangoku A, Yoshino S, Abe T, Hayashi H, Toshimitsu H, et al. Prediction of nodal metastasis by comparative genomic hybridization in biopsy specimens from patients with superficial esophageal squamous cell carcinoma. Clin Cancer Res 2003;9:5137–41.
115. Sato F, Shimada Y, Watanabe G, Uchida S, Makino T, Imamura M. Expression of vascular endothelial growth factor, matrix metalloproteinase-9 and E-cadherin in the process of lymph node metastasis in oesophageal cancer. Br J Cancer 1999;80:1366–72.
116. Kan T, Shimada Y, Sato F, Ito T, Kondo K, Watanabe G, et al. Prediction of lymph node metastasis with use of artificial neural networks based on gene expression profiles in esophageal squamous cell carcinoma. Ann Surg Oncol 2004;11:1070–8.
117. Tamoto E, Tada M, Murakawa K, Takada M, Shindo G, Teramoto K, et al. Gene-expression profile changes correlated with tumor progression and lymph node metastasis in esophageal cancer. Clin Cancer Res 2004;10:3629–38.
118. Sato T, Iizuka N, Hamamoto Y, Yoshino S, Abe T, Takeda S, et al. Esophageal squamous cell carcinomas with distinct invasive depth show different gene expression profiles associated with lymph node metastasis. Int J Oncol 2006;28:1043–55.
119. Kawamata H, Furihata T, Omotehara F, Sakai T, Horiuchi H, Shinagawa Y, et al. Identification of genes differentially expressed in a newly isolated human metastasizing esophageal cancer cell line, T.Tn-AT1, by cDNA microarray. Cancer Sci 2003;94: 699–706.

# Esophageal Cancer: Evaluation with Triple-Phase Dynamic CT—Initial Experience[1]

Shigeaki Umeoka, MD
Takashi Koyama, MD, PhD
Kaori Togashi, MD, PhD
Tsuneo Saga, MD, PhD
Go Watanabe, MD, PhD
Yutaka Shimada, MD, PhD
Masayuki Imamura, MD, PhD

**Purpose:** To prospectively assess which phase of a triple-phase dynamic contrast material–enhanced multi–detector row computed tomography (CT) protocol is optimal for visualization of esophageal cancer.

**Materials and Methods:** The study was supported by the local ethical committee; all patients gave wrjtten informed consent. Thirty-one lesions in 28 consecutive patients (26 men, two women; mean age, 65 years; range, 53–87 years) with histopathologically confirmed esophageal cancer were evaluated with triple-phase dynamic CT performed at 5, 35, and 65 seconds (first arterial, second arterial, and venous phases) after attenuation of 200 HU was obtained at the descending aorta. Qualitative image analysis was performed to assess appearance and conspicuity of the tumor. Appearances of all 31 lesions were classified into three categories—not identifiable, focal enhancement with or without minimal (<1 cm) wall thickening, and focal mass lesion or obvious (>1 cm) wall thickening. Results were compared with surgical or endoscopic ultrasonographic findings. Quantitative assessment included regions-of-interest measurement of the tumor and normal esophageal wall and the difference between those measurements. A paired $t$ test was used to determine which phase showed the highest tumor attenuation and tumor-to–normal esophageal wall attenuation differences.

**Results:** At visual assessment, 30 lesions were identified in the second arterial phase. Of these 30 lesions, eight were focal enhancements; the best conspicuity was during the second arterial phase. Furthermore, seven of these eight lesions were T1 cancers. The remaining 22 lesions were enhanced masses or wall thickening. Twenty-one of these 22 tumors also showed best conspicuity in the second arterial phase. The greatest attenuation of tumors in the second arterial phase was 130.0 HU, and the difference in attenuation between tumor and normal esophageal wall was 50.6 HU in the second arterial phase, which were significantly higher than those in the other two phases ($P < .01$, each).

**Conclusion:** The second arterial phase of dynamic CT is the optimal phase for visualization of esophageal cancer.



[1] From the Department of Diagnostic Imaging and Nuclear Medicine (S.U., K.T., T.S.) and Department of Surgery and Surgical Basic Science (G.W., Y.S., M.I.), Graduate School of Medicine, Kyoto University, Kyoto, Japan; and Department of Radiology, Kyoto University Hospital, 54 Kawahara-cho, Shogoin, Sakyo, Kyoto, 606-8507, Japan (T.K.). From the 2003 RSNA Annual Meeting. Received February 9, 2005; revision requested April 8; revision received April 28; accepted June 3; final version accepted August 11. **Address correspondence to** T.K. (e-mail: *moritpet@kuhp.kyoto-u.ac.jp*).

Esophageal cancer is one of the common malignant neoplasms in the world. Every year, approximately 13 900 cases of esophageal cancer are diagnosed in the United States, and 13 000 Americans die of it (1). Patients with esophageal cancer generally present with progressive dysphagia, malnutrition, and weight loss. As with other malignant tumors, accurate TNM staging and localization of the esophageal cancer are important parameters for selection of the optimal treatment and for prediction of patients' prognoses.

Small polypoid lesions, plaquelike lesions, focal irregularities of the esophageal wall, and spreading superficial lesions are common findings of early esophageal cancer (2,3). Because some benign esophageal tumors such as squamous papillomas can reveal similar findings, subsequent biopsy with an upper-esophageal endoscopic technique is required to confirm malignancy. A barium swallow examination typically reveals mucosal irregularity or stricture or ulceration of the esophagus. In cases of early and advanced stage esophageal cancer, the TNM stage is determined after histopathologic diagnosis in order to devise therapeutic strategies based on results of multiple imaging studies, including upper gastrointestinal endoscopy, endoscopic ultrasonography (US), computed tomography (CT), and fluorine 18 fluorodeoxyglucose positron emission tomography (4).

Because endoscopic US can depict the normal esophageal wall as a five-layer structure, it can be used to evaluate the depth of tumor extension (5). Although CT has been used for preoperative evaluation of esophageal cancer, the major role of CT has been the depiction of lymph nodes, distant metastases, or both rather than the evaluation of the local status of esophageal cancer. Several studies attempted to use conventional CT to stage esophageal cancer, only to find that CT was useful for evaluating T4 lesions (6–8). The sensitivity of conventional CT protocols in localizing esophageal cancer, especially early stage cancer, is not satisfactory, perhaps because conventional CT cannot afford optimal conspicuity of esophageal cancers against the normal esophageal wall.

**Advance in Knowledge**

- The second arterial phase of triple-phase dynamic CT is the optimal phase for visualization of esophageal cancer.

Several reports describe potential advantages of CT images obtained during the arterial phase after the administration of contrast material; these images depict gastrointestinal cancers in other organs (9–11). To our knowledge, however, this imaging technique has not been applied to esophageal cancer, as the esophagus is too long to be imaged entirely during the arterial phase at conventional CT. Multi-detector row CT has markedly improved time resolution and permits acquisition of arterial phase images of the entire esophagus during a single breath hold. Thus, the goal of our study was to prospectively assess which phase of a triple-phase dynamic contrast material–enhanced multi-detector row CT protocol is optimal for visualization of esophageal cancer.

## Materials and Methods

### Patients

Our study population included 31 lesions in 28 consecutive patients (26 men, two women; age range, 53–87 years; mean age, 65 years) with esophageal cancer histopathologically proved at endoscopic biopsy who were referred to our institution for possible surgical treatment from June 2002 to March 2003. Three patients had double primary lesions. All 28 patients underwent CT for local staging of the tumors and for evaluation of lymph nodes and distant metastases. Informed consent, which included regard to radiation dose, was obtained from all 28 patients prior to performance of triple-phase dynamic contrast-enhanced CT, in accordance with a protocol approved by the ethical committee at our institution. Anatomic subsite was divided according to Union Internationale Contre le Cancer classification: cervical esophagus, from the lower border of the cricoid cartilage to the superior thoracic aperture; upper thoracic portion, from the superior thoracic aperture to the level of tracheal bifurcation; midthoracic portion as the proximal half between the tracheal bifurcation and the esophagogastric junction; and lower thoracic portion, as the distal half between the tracheal bifurcation and the esophagogastric junction. The esophageal cancers were in the cervical esophagus in two lesions, the upper thoracic portion in five lesions, the midthoracic portion in eight lesions, both the upper thoracic and midthoracic portions in three lesions, the lower thoracic portion in five lesions, and both the midthoracic and lower thoracic portions in eight lesions. Histopathologic diagnoses were squamous cell carcinoma (30 lesions, 27 patients) and adenocarcinoma arising in a Barrett esophagus (one lesion, one patient). Treatments were the following: surgical resection for 15 lesions in 14 patients, radiation therapy or combined chemotherapy and radiation therapy for seven lesions in five patients, endoscopic mucosal resection for one lesion in one patient, and combination of surgical resection with radiation therapy, chemotherapy, or both in eight lesions in eight patients. The local extent of the primary tumor (T classification) was determined with histopathologic assessment of the resected specimens (23 lesions) according to the TNM classification. For the eight lesions without surgical interven-

**Published online before print**
10.1148/radiol.2393050222

**Radiology 2006**; 239:777–783

**Abbreviation:**
ROI = region of interest

**Author contributions:**
Guarantor of integrity of entire study, T.K.; study concepts/study design or data acquisition or data analysis/interpretation, all authors; manuscript drafting or manuscript revision for important intellectual content, all authors; approval of final version of submitted manuscript, all authors; literature research, S.U., T.K., K.T.; clinical studies, all authors; statistical analysis, S.U.; and manuscript editing, S.U., T.K., K.T., T.S., M.I.

Authors stated no financial relationship to disclose.

tions, results from endoscopic US were used as the reference standard for diagnosis. The criteria for staging with endoscopic US evaluation were based on the classification system for the esophagus as proposed by the Japanese Society for Esophageal Diseases (12,13).

### Dynamic CT Protocol

All examinations were performed with the same multi-detector row CT scanner (Aquilion M8; Toshiba Medical, Tokyo, Japan). CT scans were obtained after intravenous injection of 100 mL of nonionic contrast medium (350 or 370 mg of iodine per milliliter) (Iomeprol, Eisai, Tokyo, Japan; Iopamidol, Nihon Schering, Osaka, Japan) at a rate of 3 mL/sec. Triple-phase imaging with a single breath hold for each phase was automatically performed 5, 35, and 65 seconds (first arterial phase, second arterial phase, and venous phase) after the attenuation of the descending aorta reached 200 HU. The first and second arterial phase acquisitions covered from the neck to the level of the esophagogastic junction, whereas the venous phase acquisitions covered the whole abdominal and pelvic region, in addition to the neck and chest region. Thirty-second intervals were allowed between each phase (15 seconds to obtain images of the entire length of the esophagus and another 15 seconds for patients to recover their breath). Oral esophageal contrast material was not used in this study, because esophageal enhancement may be confused with tumor enhancement on images.

Images were acquired with 1- or 2-mm section thickness, beam collimation of 8, 556-msec rotation time, beam pitch of 1.7 or 0.875, 120 kVp, 300 mA per rotation, and 14-mm table feed per rotation. The thin-section CT data were transferred to a workstation (M900 Quadra; Ziosoft, Tokyo, Japan), and transverse 7.0-mm-thick sections were reconstructed at 7.0-mm intervals. The reconstruction field of view was 320 mm for each section. Multiplanar reformatted images were also reconstructed by one of the authors (S.U., with approximately 5 years of experience in thoracic and abdominal CT) with a 1.0-mm section thickness in the oblique sagittal plane, which included the tumor and either the trachea (in cases of cervical or upper thoracic esophageal cancers) or the descending aorta (in cases of midthoracic or lower thoracic esophageal cancers). Standard mediastinal window images (window width, 400 HU; window level, 60 HU) were used for displaying the images.

### Qualitative Analysis

Qualitative image analysis was prospectively performed on both transverse CT images and multiplanar reformatted CT images by two radiologists (T.K. and T.S., each with approximately 9 years of experience in thoracic and abdominal CT) who were aware of the histopathologic diagnosis of esophageal cancer but had no information on numbers and location of the tumor described in the surgical and US endoscopic findings. These readers assessed the images for the presence of the tumor, which is noted as focal enhancement. When the tumor was identified, each reader recorded the location and thickness of the lesion. Discrepancies in assessment were solved by consensus. For each imaging phase, appearances of all 31 lesions were classified into the following three categories: not identifiable (type 1), focal enhancement with or without minimal (<1 cm) wall thickening (type 2), and focal mass lesion or obvious (>1 cm) wall thickening (type 3).

Visual assessment of the phase that best showed the tumor against normal esophageal wall was also performed by using a five-point scale: 1, nonidentifiable; 2, hardly identifiable; 3, adequate; 4, good; and 5, excellent. Conspicuity of a type 1 lesion was equivalent to a score of 1. Conspicuity of type 2 or 3 lesions was ranked according to scores 2–5.

**Table 1**

**Appearance of 31 Esophageal Tumors on Triple-Phase CT Images, according to Imaging Phase**

| Appearance of Esophageal Tumors | No. of Detectable Lesions | | |
|---|---|---|---|
| | First Arterial Phase | Second Arterial Phase | Venous Phase |
| Not identifiable (type 1) | 9 | 1 | 7 |
| Focal enhancement with or without minimal (<1 cm) wall thickening (type 2) | 0 | 8 | 2 |
| Focal mass lesion or obvious (>1 cm) wall thickening (type 3) | 22 | 22 | 22 |

**Table 2**

**Best Esophageal Tumor Conspicuity on Triple-Phase CT Images, according to Imaging Phase**

| Appearances of Esophageal Tumors | Best Conspicuity | | | |
|---|---|---|---|---|
| | First Arterial Phase | Second Arterial Phase | Venous Phase | Both Second and Venous Phases |
| Focal mass lesion or obvious (>1 cm) wall thickening (type 3) ($n$ = 22) | 0 | 10 | 1 | 11 |
| Focal enhancement with or without minimal (<1 cm) wall thickening (type 2) ($n$ = 8) | 0 | 8 | 0 | 0 |

Although histopathologic confirmations were not obtained, linear or punctuate enhancements along the surface mucosa were considered to be physiologic mucosal enhancement or vessels. These enhanced structures were carefully excluded. High attenuation due to beam hardening artifacts at the interface between the esophageal lumen and the esophageal wall were also carefully excluded. The locations of the esophageal cancers at CT assessment were finally compared with surgical or endoscopic findings by another author (S.U.).

### Quantitative Analysis

In parallel with qualitative analyses, quantitative analyses were performed by another radiologist (S.U.) who was aware of the tumor locations from endoscopic US or surgical results. The mean attenuations of the esophageal tumor and of the normal esophageal wall were measured in Hounsfield units within three circular regions of interest (ROIs), which were created as large as possible on both the cancerous and the normal esophageal wall on the transverse image. The average of the three measurements was calculated as attenuation of the tumor and attenuation of the normal esophageal wall. When defining all ROIs, the radiologist paid special attention not to include necrosis within the tumor, linear enhancement along the surface mucosa, esophageal contents, fat tissue, or surrounding vessels. If the tumor was not identifiable during one or two imaging phases, the ROI was defined by referring to images of another phase that showed the location of the lesion.

### Data and Statistical Analysis

Tumor locations and appearances interpreted from the CT images were compared with surgical and endoscopic US findings. The differences in CT attenuation between the tumor and the normal esophageal wall were calculated as an indicator of visual conspicuity of the lesion. Both attenuation of the tumors and subtracted tumor-to–normal esophageal wall attenuation differences were compared between images from different phases. Paired *t* tests were performed with statistical software (Stat View version 5.0.1; SAS Institute, Cary, NC). Because data were accumulated over time, a repeated measurement distribution analysis was carried out. Compensation of the multiplex nature was performed by the Tukey method. A *P* value of less than .05 was considered to indicate a statistically significant difference.

## Results

### Staging

The local endoscopic US or surgical staging of the 31 lesions included T1 cancer in nine lesions (one T1a, eight T1b), T2 cancer in five lesions, T3 cancer in 12 lesions, and T4 cancer in five lesions.

**Figure 1**

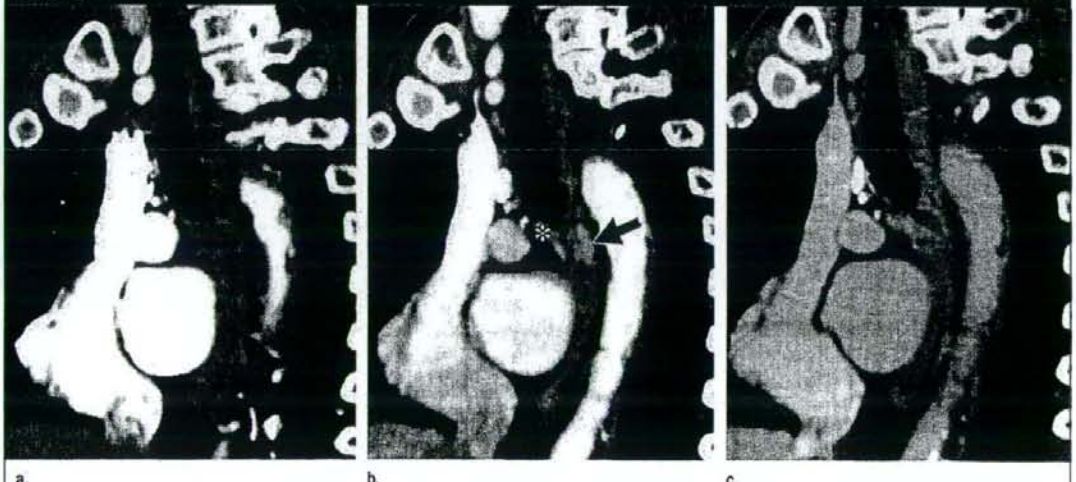

a. b. c.

**Figure 1:** Oblique sagittal reformatted CT images of 72-year-old man with submucosal esophageal cancer (T1b cancer) 20 × 15 mm in diameter in midthoracic portion. **(a)** First arterial phase image shows smooth esophageal walls without any abnormal enhancement. **(b)** Second arterial phase image reveals focal enhancement (arrow) about 8 mm in diameter and 15 mm in length without any wall thickening (approximately 9 mm thick). Image provides best conspicuity among three phases. Subcarinal adenopathy is seen (*). **(c)** Venous phase image does not show abnormality as well. Average attenuation of tumor is 82 HU in first arterial phase, 129 HU in second arterial phase, and 97 HU in venous phase. Difference in attenuation between tumor and esophageal wall is 10 HU in first arterial phase, 49 HU in second arterial phase, and 5 HU in venous phase.

**Figure 2**

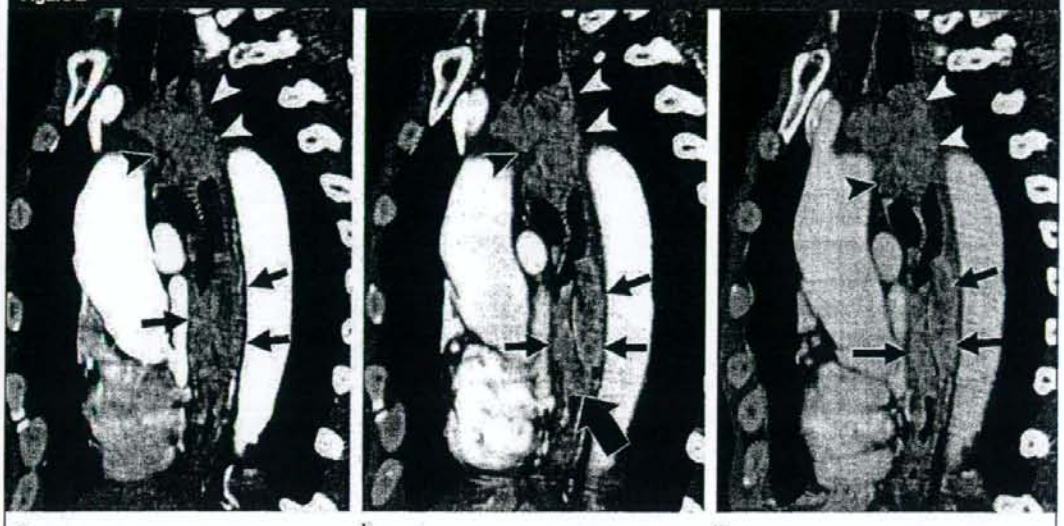


**Figure 2:** Oblique sagittal reformatted CT images of 55-year-old man with T3 tumor of 5.5 cm in diameter in midthoracic portion (small arrows) and T3 tumor of 7.0 cm in diameter in upper thoracic portion (arrowheads). **(a)** First arterial phase image demonstrates tumors in upper and midthoracic portions. **(b)** Second arterial phase image displays an early attenuation of lesions and provides best conspicuity of tumor among the three phases. Lower edge of tumor is clearly identifiable on image (large arrow). **(c)** Venous phase image shows tumors with less conspicuous margins compared with second arterial phase image. Average attenuations of upper thoracic and midthoracic tumors are 83 HU and 89 HU in first arterial phase, 129 HU and 116 HU in second arterial phase, and 116 HU and 112 HU in venous phase, respectively. Tumor-to–normal esophageal wall attenuation differences are 28 HU and 34 HU in first arterial phase, 64 HU and 66 HU in second arterial phase, and 44 HU and 40 HU in venous phase, respectively.

### Qualitative Analysis

The presence of all esophageal cancers depicted at CT had been correctly determined from the surgical specimens or endoscopic US. At CT, thirty lesions (97%), which included three skip lesions, were identifiable in the second arterial phase, whereas 22 lesions (71%) were identifiable in the first arterial phase and 24 lesions (77%) were identifiable in the venous phase (Table 1). Only one lesion (type 1) was not identifiable at CT during any of the three phases; this lesion was an adenocarcinoma arising in a Barrett esophagus. At histopathologic examination, the tumor was confined to the mucosal layer within the Barrett epithelium (T1a cancer). The mean wall thickness of the 30 identifiable tumors was 12 mm.

The appearances of eight lesions were interpreted as type 2 cancers on second arterial phase images. Seven of these eight lesions (88%) were histopathologically diagnosed as T1b tumors, whereas the remaining lesion was diagnosed as T2 cancer. Of these eight lesions, none were identifiable in the first arterial phase, and only two lesions were depicted in the venous phase. All eight lesions were depicted most conspicuously in the second arterial phase (Table 2), and six lesions were identifiable only in the second arterial phase (Fig 1).

Twenty-two lesions had type 3 appearances and were identifiable in all three phases (Fig 2). These 22 lesions consisted of one T1b lesion, four T2 lesions, 12 T3 lesions, and five T4 lesions. In 21 of 22 lesions (95%), the best conspicuity between the tumor and the normal esophageal wall was obtained in the second arterial phase (Table 2). The mean wall thickness of eight type 2 lesions was 6.3 mm, whereas that of the 22 type 3 lesions was 13 mm.

### Quantitative Analysis

In 28 of 31 lesions, attenuation was measured. In the remaining three lesions, attenuation could not be measured because one lesion was not identifiable in all three phases and the remaining two lesions were too small to define ROIs within the tumors. The mean attenuation of the esophageal tumor was statistically highest in the second arterial phase ($P < .01$ compared with both the first arterial and the venous phases) (Table 3). With regard to the attenuation difference between the tumor and normal esophagus wall, the second arterial phase also showed significantly better conspicuity than both the first arterial and the venous phases ($P < .01$). The mean attenuation of the esophageal tumor showed a peak in the second arterial phase, while the attenuation of the normal esophageal wall tended to gradually enhance (Fig 3).

The mean tumor-to-normal esophageal wall attenuation difference was greatest in the second arterial phase.

## Discussion

At conventional CT with contrast material enhancement, images are acquired in the venous phase, and esophageal cancer can be demonstrated in approximately 80% of lesions (14). This frequency of demonstration is nearly equivalent to that in the venous phase in our study (24 of 31 [77%]). Missed cancers at CT may result from poor delineation of early stage cancers without obvious wall thickening. Yoon et al reported that 69.2% of T1 lesions were not demonstrated at CT (14). At conventional CT, identification of esophageal cancers usually depends on wall thickening of the esophagus (15). Early stage cancers, however, may show minimal or no wall thickening. Wu et al (16) proposed a classification of tumor staging: Cancers with thickness greater than 5 mm and less than 15 mm are considered modified T2, those with thickness greater than 15 mm and with an irregular outer margin are considered T3, and tumor invasion of adjacent organs is considered T4. However, Wu et al had no criteria for T1 lesions because T1 lesions cannot be delineated by the thickness of the wall alone.

Our results showed that with dynamic CT, the second arterial phase is the optimal phase for visualization. Cancers in the second arterial phase can be identified as enhanced foci, even if the cancer does not cause wall thickening. As for advanced stage cancers with wall thickening, the second arterial phase most clearly depicts the tumors. These results are also supported by quantitative analysis of the difference in attenuation between the tumor and normal esophageal wall. Esophageal cancer shows a peak of enhancement around the second arterial phase, whereas normal esophageal wall shows gradual enhancement. Therefore, the best conspicuity of esophageal cancer against the esophageal wall can be obtained at this time.

Although the venous phase images seem inferior to the second arterial phase images with regard to the representation of esophageal cancer, venous phase images may be useful in evaluating mediastinal lymphadenopathy. In addition, by analyzing the venous phase images of the esophagus, multi-detector row CT can allow rapid imaging of the abdomen for the purpose of screening distant metastases and lymphadenopathy. In the evaluation of liver metastasis, liver parenchyma is not enhanced enough at the arterial phases and may not be adequate for depicting lesions other than hypervascular tumors, such as hepatocellular carcinoma (17). The first arterial phase images may have no clinical value in the evaluation of esophageal cancer and metastatic lesions. Ideally, both the second arterial and the venous phase images are required for the evaluation of esophageal cancers; however, increasing the number of scans causes increased radiation dose.

Improved delineation of esophageal cancer at multi-detector row CT can provide several potential clinical benefits. Precise localization of esophageal cancer is useful for planning radiation therapy or surgical resection. Once chemotherapy or radiation therapy is chosen, clear delineation of the tumor as an enhanced lesion may be useful for evaluating the therapeutic outcome. Moreover, clear delineation of esophageal cancer may improve recognition of relationships to the adjacent mediastinal organs and thus improve accuracy of local staging of the tumors.

There were some limitations in our study. First, the number of adenocarcinomas and T1a cancers was very limited in our population. The only case of adenocarcinoma in our study was a mucosal cancer (T1a cancer), and it was not demonstrated at CT. T1a cancer may not be delineated, even with dynamic CT. In such instances, the presence of enhanced lesions within nonthickened walls may become a useful radiologic feature that allows the differentiation of T1b cancers from T1a cancers, although further evaluation is required with early stage cases. Esophageal adenocarcinomas of advanced stages may show radiologic features and enhancing patterns that are different from those of squamous cell carcinomas. Although the prevalence of adenocarcinomas in Japan is increasing, the proportion of adenocarcinomas to squamous cell carcinomas is still low and differs from that in the United States

**Figure 3**

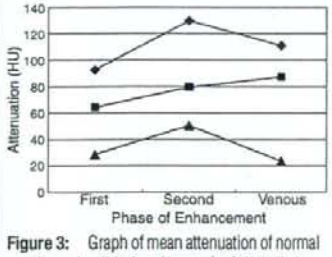


**Figure 3:** Graph of mean attenuation of normal esophageal wall (■) and tumor (◆). Note that attenuation of tumor and tumor-to–normal esophageal wall attenuation differences (▲) peak in second arterial phase, whereas attenuation of esophageal wall elevates gradually.

**Table 3**

**Mean Attenuation of 28 Esophageal Tumors, Normal Esophageal Walls, and the Difference between Them**

| CT Imaging Phase | Mean Attenuation of Tumor (HU) | Mean Attenuation of Normal Esophageal Wall (HU) | Mean Tumor-to–Normal Esophageal Wall Attenuation Difference (HU) |
|---|---|---|---|
| First arterial | 92.5 ± 14.7 | 64.2 ± 15.8 | 28.3 ± 17.1 |
| Second arterial | 130.0 ± 18.4 | 79.4 ± 20.6 | 50.6 ± 23.0 |
| Venous | 111.0 ± 13.7 | 87.2 ± 16.5 | 23.5 ± 19.0 |

(18). Further evaluation is required to investigate whether this technique is applicable for patients with adenocarcinoma.

Second, our study population included only patients with esophageal cancer and did not consist of any healthy subjects because of radiation exposure. The readers were not blinded for the presence of the tumor. Hence, it is questionable whether this technique is useful in screening for esophageal cancer. In patients with inflammatory diseases, including gastroesophageal reflux disease or Barrett esophagus, CT appearances of these diseases may resemble early stage esophageal cancers (19). Distribution of inflammatory lesions, however, would be usually more superficial and diffuse than that of cancers.

Third, qualitative evaluation of CT images from all three phases was performed on the same day in our study, which may cause bias. We are convinced, however, that the results from quantitative analysis support reproducibility of qualitative analysis.

In conclusion, the results of our study show that the second arterial phase of dynamic CT is the optimal phase for visualization of esophageal cancer.

Acknowledgment: The authors thank Hiroto Hatabu, MD, PhD, Department of Radiology, Beth Israel Deaconess Medical Center, Harvard Medical School, Boston, Mass, for his guidance in the preparation of the manuscript.

## References

1. Jemal A, Tiwari RC, Murray T, et al. Cancer statistics, 2004. CA Cancer J Clin 2004;54:8–29.
2. Levine MS. Esophageal cancer: radiologic diagnosis. Radiol Clin North Am 1997;35:265–279.
3. Kumbasar B. Carcinoma of esophagus: radiologic diagnosis and staging. Eur J Radiol 2002;42:170–180.
4. Rankin SC, Taylor H, Cook GJ, Mason R. Computed tomography and positron emission tomography in the pre-operative staging of oesophageal carcinoma. Clin Radiol 1998;53:659–665.
5. Whyte RI. Advances in the staging of intrathoracic malignancies. World J Surg 2001;25:167–173.
6. Quint LE, Glazer GM, Orringer MB, Gross BH. Esophageal carcinoma: CT findings. Radiology 1985;155:171–175.
7. Picus D, Balfe DM, Koehler RE, Roper CL, Owen JW. Computed tomography in the staging of esophageal carcinoma. Radiology 1983;146:433–438.
8. Vilgrain V, Mompoint D, Palazzo L, et al. Staging of esophageal carcinoma: comparison of results with endoscopic sonography and CT. AJR Am J Roentgenol 1990;155:277–281.
9. Lee JH, Jeong YK, Kim DH, et al. Two-phase helical CT for detection of early gastric carcinoma: importance of the mucosal phase for analysis of the abnormal mucosal layer. J Comput Assist Tomogr 2000;24:777–782.
10. Mani NB, Suri S, Gupta S, Wig JD. Two-phase dynamic contrast-enhanced computed tomography with water-filling method for staging of gastric carcinoma. Clin Imaging 2001;25:38–43.
11. Hundt W, Braunschweig R, Reiser M. Evaluation of spiral CT in staging of colon and rectum carcinoma. Eur Radiol 1999;9:78–84.
12. Dittler HJ, Pesarini AC, Siewert JR. Endoscopic classification of esophageal cancer: correlation with the T stage. Gastrointest Endosc 1992;38:662–668.
13. Japanese Gastric Cancer Association. Japanese classification of gastric carcinoma: 2nd English edition. Gastric Cancer 1998;1:10–24.
14. Yoon YC, Lee KS, Shim YM, Kim BT, Kim K, Kim TS. Metastasis to regional lymph nodes in patients with esophageal squamous cell carcinoma: CT versus FDG PET for presurgical detection prospective study. Radiology 2003;227:764–770.
15. Koehler RE, Memel DS, Stanley RJ. Gastrointestinal tract. 3rd ed. In: Lee JKT, Sagel SS, Stanley RJ, Heiken JP, eds. Computed tomography with MRI correlation. Philadelphia, Pa: Lippincott-Raven, 1998; 637–700.
16. Wu LF, Wang BZ, Feng JL, et al. Preoperative TN staging of esophageal cancer: comparison of miniprobe ultrasonography, spiral CT and MRI. World J Gastroenterol 2003;9:219–224.
17. Hori M, Murakami T, Kim T, Tomoda K, Nakamura H. CT scan and MRI in the differentiation of liver tumors. Dig Dis 2004;22:39–55.
18. Hongo M. Review article: Barrett's oesophagus and carcinoma in Japan. Aliment Pharmacol Ther 2004;20(suppl 8):50–54.
19. Berkovich GY, Levine MS, Miller WT Jr. CT findings in patients with esophagitis. AJR Am J Roentgenol 2000;175:1431–1434.

*Int. J. Cancer:* **118**, 230–242 (2006)


# Cisplatin-dependent upregulation of death receptors 4 and 5 augments induction of apoptosis by TNF-related apoptosis-inducing ligand against esophageal squamous cell carcinoma

**Kan Kondo[1]*, Seiji Yamasaki[2], Tomoharu Sugie[3], Naoki Teratani[1], Takatsugu Kan[1], Masayuki Imamura[1] and Yutaka Shimada[1]**

[1]*Department of Surgery and Surgical Basic Science, Graduate School of Medicine, Kyoto University, Kyoto, Japan*
[2]*Department of Surgery, Murakami Memorial Hospital, Gifu prefecture, Japan*
[3]*Department of Surgery, Kyoto Police Hospital, Kyoto, Japan*

**TNF-related apoptosis-inducing ligand (TRAIL) is a member of the TNF superfamily known to induce apoptosis in a variety of cancers. The purpose of our study was to examine the effects of TRAIL in combination with cisplatin against esophageal squamous cell carcinoma (ESCC) cell lines *in vitro* and *in vivo*, and to elucidate underlying molecular mechanisms. Expression profiles of TRAIL receptors were investigated in 19 ESCC (KYSE) cell lines using RT-PCR. Crystal violet staining assays were performed to reveal the sensitivity against TRAIL. Flow cytometric analyses of apoptosis induction and TRAIL receptor expression were performed. Furthermore, Western blot was used to clarify the apoptosis pathway involved, and a nude-mouse xenograft model was used to show effects *in vivo*. Results show that death receptors (DR) 4 and 5 were expressed in 100% of the cell lines, and 79% (15/19) expressed 4 TRAIL receptors. There was only 1 cell line without decoy receptor expression. Eighteen cell lines were resistant to TRAIL, but in some, the combination treatment with cisplatin could overcome this resistance. They underwent apoptosis *via* activation of caspase-8 and -3, and cisplatin-dependent upregulation of DR4 and 5 was detected. Furthermore, pretreatment with cisplatin followed by TRAIL resulted in significant tumoricidal effects. Finally, systemic administration of TRAIL with cisplatin synergistically suppressed tumor growth of ESCC xenografts in nude mice. These results provide a significance of cisplatin-induced upregulation of death receptors as apoptosis-inducing machinery, and it was suggested that sequential administration of cisplatin and TRAIL might be a feasible chemotherapeutic regimen against ESCC.**


**Key words:** TNF-related apoptosis-inducing ligand (TRAIL); apoptosis; cisplatin; esophageal squamous cell carcinoma; chemotherapy

Esophageal SCC has extremely poor prognosis among gastrointestinal cancers because the diagnosis is not made until at an advanced stage and there are few effective therapies. Esophagectomy with extensive lymphadenectomy is far from being satisfactory with a dismal 5-year survival rate, and available chemotherapeutic regimens are yet to show promising outcomes. Thus, we are still in the midst of searching for a more effective modality to conquer this highly mortal malignancy.

TRAIL (also known as Apo2L) is a relatively new member of the TNF family that has been discovered from the expression sequence tag.[1,2] TRAIL is highly homologous to FasL and other members of the TNF ligand family, and its constitutive expression has been detected in a variety of human tissues including spleen, thymus, prostate, peripheral blood lymphocytes, ovary, small intestine, colon, placenta and lung, but not in the brain, liver or testis.[1] Four cognate receptors have been identified: death receptor (DR) 4 (TRAIL receptor (TR) 1)[3] and DR5 (KILLER/TR2[4–6] are receptors with fully functional cytoplasmic death domains. On the other hand, decoy receptor (DcR) 1 (TRID / TR 3)[4–6] and DcR 2 (TRUNDD / TR 4)[9–11] have either an obliterated (DcR1) or a truncated (DcR2) death domain. These decoy receptors have been proposed to competitively inhibit TRAIL-induced apoptosis by acting as nonfunctional receptors. All 4 TRAIL receptors are highly expressed in a wide variety of normal cells and the expression of decoy receptors is substantially limited in tumor cells.[3,5,10] These findings in addition to normal cells' resistance to TRAIL have lead to the presumptive belief that normal cells are protected from TRAIL-mediated apoptosis by decoy receptors[1,2,4,6,9,10] However, later studies revealed that DcR1 and DcR2 are also expressed in some cancers sensitive to TRAIL, thereby defying their putative function[12–15] Currently, exact functions of decoy receptors remain unknown and the mechanism for normal cells' resistance to TRAIL is still obscure. In the meantime, some studies raised questions regarding toxicity of TRAIL against normal tissues,[12,16] but this controversy seemed to be resolved by further findings that clinical-grade recombinant human TRAIL has minimal toxicity against normal human cells.[17,18]

Although TRAIL has been shown to be capable of inducing apoptosis in tumor cells of diverse origin,[19–23] studies on esophageal cancer have been very rare. In our study, ESCC cell lines (KYSE series) that have been established at our institution[24,25] are subjected to a series of experiments to demonstrate the potential usefulness of TRAIL against ESCC and underlying mechanisms behind this therapeutic model is discussed.

## Material and methods

### *Cell lines*

Nineteen genetically distinct KYSE cell lines were used. HeLa cells were used as positive controls for surface expression of DR4 and DR5 in flow cytometry. Peripheral blood mononuclear cells (PBMCs) isolated from whole blood of 2 of the authors (KK and NT) using Ficoll-Paque solution (Amersham Biosciences, London, UK) served as normal controls. All cells were cultured and maintained in RPMI 1640 (Nikken Biomedical Laboratory, Kyoto, Japan) plus 2% Fetal Bovine Serum (Biofluids, MD) at 37°C, in humidified 5% $CO_2$ atmosphere.

### *Patients*

Original ESCC from which 19 KYSE series were established had been obtained during esophagectomy performed at the Department of Surgery and Surgical Basic Science of Kyoto University. All patients had a pathological diagnosis of squamous cell carcinoma, and their histological grading and staging were classified according to the pathological tumor/node/metastasis (pTNM) system (5th edition). The subjects consisted of 16 men and 3 women of age, 39–79 years (average age of 57.7 ± 9.8 years). There were no patients with distant organ metastasis, so all of the stage IV patients had distant lymph node metastasis. Details of patient characteristics are displayed in Table I. Written consent was obtained from the patients for the performance of surgery and for the use of

***Correspondence to:** Department of Surgery and Surgical Basic Science, Graduate School of Medicine, Kyoto University, Shogoin Kawaharacho 54, Sakyo-ku, Kyoto 606-8507, Japan. Fax: +81-75-751-4390 or +81-75-862-2312. E-mail: Terurin@kuhp.kyoto-u.ac.jp
Received 8 December 2004; Accepted after revision 27 April 2005
DOI 10.1002/ijc.21283
Published online 7 July 2005 in Wiley InterScience (www.interscience.wiley.com).

TABLE 1 – CLINICOPATHOLOGICAL CHARACTERISTICS OF 19 ORIGINAL TUMORS[1]

| Parameter | n | Sensitivity to combination Tx | | p Value |
|---|---|---|---|---|
| | | + | – | |
| Age (years) | | | | |
| <50 | 3 | 1 | 2 | >0.999 |
| >50 | 16 | 6 | 10 | |
| Sex | | | | |
| Female | 4 | 2 | 2 | = 0.603 |
| Male | 15 | 5 | 10 | |
| N status | | | | |
| N(+) | 16 | 5 | 11 | = 0.523 |
| N(−) | 3 | 2 | 1 | |
| M status | | | | |
| M(+) | 5 | 2 | 3 | >0.999 |
| M(−) | 14 | 5 | 9 | |
| Tumor location | | | | |
| Ce | 4 | 1 | 3 | = 0.930 |
| Ut | 3 | 1 | 2 | |
| Mt | 10 | 4 | 6 | |
| Lt | 2 | 1 | 1 | |
| TNM stage | | | | |
| 2a | 3 | 2 | 1 | = 0.640 |
| 2b | 2 | 0 | 2 | |
| 3 | 9 | 3 | 6 | |
| 4a | 2 | 1 | 1 | |
| 4b | 3 | 1 | 2 | |
| Histological differentiation | | | | |
| Well | 6 | 1 | 5 | = 0.365 |
| Moderate | 8 | 4 | 4 | |
| Poor | 4 | 2 | 2 | |

[1]Values represent numbers of patients except otherwise indicated.

resected samples for research in accordance with the Kyoto University Institutional Review Board.

*Cytokines and antibodies*

Soluble recombinant human TRAIL was purchased from DAKO (Denmark); cisplatin was obtained from Nippon Kayaku Co. Ltd. (Tokyo, Japan). Monoclonal mouse anti-caspase-8, anti-human BAX, anti-FADD and anti-XIAP antibodies were purchased from Medical & Biological Laboratories Co., Ltd (Nagoya, Japan). A monoclonal mouse anti-Bcl-X antibody, and polyclonal rabbit anti-caspase-8 and anti-caspase-3 antibodies were purchased from BD Pharmingen (San Diego, CA). A polyclonal rabbit anti-cFLIP antibody, a monoclonal mouse anti-β-actin antibody, and a mouse IgG1 isotype control were purchased from Sigma-Aldrich, Inc. (St. Louis, MO). A monoclonal mouse anti-FLIP antibody was purchased from Apotec (Geneva, Switzerland). Rabbit polyclonal anti-NFκB antibodies (anti-p50 and anti-p65) were purchased from Santa Cruz Biotechnology, Inc. (Santa Cruz, CA). Peroxidase-conjugated sheep anti-mouse IgG and donkey anti-rabbit IgG were purchased from Amersham Pharmacia Biotech (London, UK). Monoclonal mouse antibodies to TRAIL-R1, -R2, -R3, and -R4, and a biotinylated polyclonal antibody to mouse IgG1, were purchased from Alexis Biochemicals (UK). Streptavidin/FITC was purchased from Ancell Corporation (Bayport, MN).

*Total RNA extraction and RT-PCR*

Total RNA from KYSE cell lines was extracted using TRIzol reagent (Invitrogen, Carlsbad, CA) in accordance with the manufacturer's recommendations. PBMCs were incubated overnight in a 6-well tissue culture plate (Iwaki glass, Tokyo, Japan) before total RNA extraction. RNA quantification was performed spectrophotometrically. First strand cDNA was synthesized using 1 μg of total RNA, 1 μl of oligo $dT_{(12-18)}$ (Invitrogen), 4 μl of 5× first strand buffer (Invitrogen), 4 μl of dNTP mix (2.5 mM each) (Invitrogen) and 2 μl of 0.1 M DTT (Invitrogen), in a total volume of 20 μl. Previously published sequences of PCR primers were adopted: DR4 sense, 5′-CTG-AGC-AAC-GCA-GAC-TCG-CTG-TCC-AC-3′; DR4 antisense, 5′-AAG-GAC-ACG-GCA-GAG-CCT-GTG-CCA-T-3′;[26] DR5 sense, 5′-CTG-AAA-GGC-ATC-TGC-TCA-GGT-G-3′; DR5 antisense, 5′-CAG-AGT-CTG-CAT-TAC-CTT-CTA-G-3′[19] DcR1 sense, 5′-GTT-TGT-TTG-AAA-GAC-TTC-ACT-GTG-3′; DcR1 antisense, 5′-GCA-GGC-GTT-TCT-GTC-TGT-GGG-AAC-3′;[13] DcR2 sense, 5′-CTT-TTC-CGG-CGG-CGT-TCA-TGT-CCT-TC-3′; DcR2 antisense, 5′-GTT-TCT-TCC-AGG-CTG-CTT-CCC-TTT-GTA-G-3′;[26] glyceraldehyde-3-phosphate dehydrogenase (GAPDH) sense, 5′-TGG-TAT-CGT-GGA-AGG-ACT-CAT-GAC-3′ and GAPDH antisense, 5′-ATG-CCA-GTG-AGC-TTC-CCG-TTC-AGC-3′. PCR was performed using 5 μl of 10× PCR buffer (Sawady Technology, Tokyo, Japan), all 4 dNTPs at 2.5 mM, 2.5 U Taq DNA polymerase (Sawady Technology), 1/20 of cDNA and each primer at 0.5 μM, in a total volume of 50 mgr;l using PTC-200 Peltier thermal cycler (MJ Research, Inc., Watertown, MA). Thirty-five cycles of amplification were performed (melting step at 94°C for 1 min (DR4), 45 sec (DR5), 30s (DcR1), and 45 sec (DcR2); annealing step at 62°C for 1 min (DR4), 57°C for 45 sec (DR5), 56°C for 30 sec (DcR1), and 63°C for 45 sec (DcR2); elongation step at 72°C for 1 min (DR4), 45 sec (DR5), 30 sec (DcR1) and 45 sec (DcR2); followed by a final step at 72°C for 10 min). PCR product lengths were 505 bp (DR4), 583 bp (DR5), 140 bp (DcR1), 464 bp (DcR2) and 189 bp (GAPDH). Samples without reverse transcriptase served as negative controls to confirm that there was no genomic DNA contamination.

*Crystal violet staining assay*

Each cell line was cultured until subconfluent in 12-well tissue culture plates (Iwaki glass), and TRAIL (0 ng/ml, 50 ng/ml or 100 ng/ml) and cisplatin (0 μg/ml, 2.5 μg/ml or 5 μg/ml) were added either alone or in combinations for 24 hr. Then medium was discarded and adherent cells were washed with PBS, stained and fixed with 0.2% crystal violet in 10% phosphate-buffered formaldehyde (Wako Pure Chemical, Japan) for 30 sec. Excess crystal violet solution was discarded, and adherent cells, considered viable, were observed. After completely air-dried, stained cells were lysed with 2% SDS solution by shaking plates in room temperature for 1 hr. OD absorbance was measured at 560 nm using SJeia II microplate reader (Sanko Jun-yaku Co., Ltd., Tokyo, Japan), and the percent absorbance of every well was determined.

*Flow cytometry for detection of apoptotic cells and surface TRAIL receptor expression*

KYSE cell lines, HeLa cell line ($5 \times 10^5$ cells) and PBMCs ($3 \times 10^6$ cells) were seeded in 24-well tissue culture plates (Iwaki glass). For detection of apoptosis, TRAIL (50 ng/ml) and cisplatin (5 μg/ml) were added either alone or in combination for 24 hr. Subsequently, floating cells in the medium and adherent cells were collected. Using Annexin V-FITC Apoptosis Detection Kit (Medical & Biological Laboratories Co., Ltd.), cells were stained with Annexin-V FITC and propidium iodide (PI) according to manufacturer's instructions. Untreated cells and cells treated with 3% formaldehyde for 30 min served, respectively, as negative and positive controls for double staining. For detection of surface TRAIL receptor expression, cells were either untreated (control) or treated with 5 μg/ml cisplatin for 6 hr, harvested, and stained with monoclonal antibodies against TR1–TR4, followed sequentially by incubation with biotinylated goat anti-mouse IgG, and then with streptavidin-FITC. HeLa cells served as positive controls for DR4/5 surface expression, and PBMCs served as positive controls for DcR1/2 surface expression. Cells were analyzed immediately after staining using a FACScan flow cytometer (Becton Dickinson, Mountain View, CA) and the Cell Quest software (Becton Dickinson). For each measurement, >10,000 cells were counted.

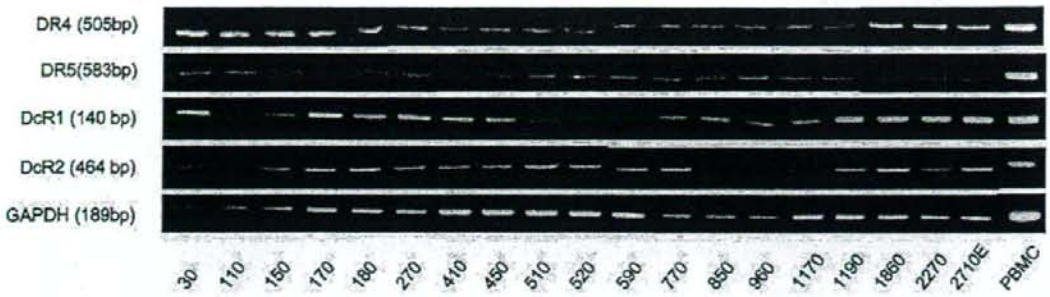


FIGURE 1 – RT-PCR detection of TRAIL receptors in 19 KYSE cell lines and peripheral blood mononuclear cells (PBMCs): RT-PCR was run for 35 cycles. DR4 and DR 5 were expressed in all cell lines. Four cell lines lacked DcR2 expression, and KYSE 110 was the only decoy receptor (−) cell line. Glyceraldehyde-3-phosphate dehydrogenase (GAPDH) expression is shown as a loading control. Experiments were repeated at least 3 times and the most representative results are shown.

*Morphological analysis using Hoechst33342 and propidium iodide staining*

In some cell lines, nuclear morphology was assessed using Hoechst 33342 and PI staining. After 24 hr treatment with TRAIL and cisplatin, cells were harvested, labeled with Hoechst 33342 (5 μg/ml) and PI (1 μg/ml) at 37°C for 10 min and examined under fluorescent microscopy according to the method reported previously.[27] Intact blue nuclei, condensed/fragmented blue nuclei, condensed/fragmented pink nuclei and intact pink nuclei were considered viable, early apoptotic, late apoptotic and necrotic cells, respectively.

*Immunoblotting analyses*

Lysis buffer containing 2% SDS solution supplemented with Tris-HCl, pH 6.5 and 25% glycerol, and a mixture of protease inhibitors in DMSO solution (Wako Pure Chemicals) was used to destruct cellular structures. Lysates were then sonicated on ice, centrifuged and protein concentration determined using BCA protein assay kit (Pierce, Rockford, IL). Next, Sodium dodecyl sulfate-polyacrylamide gel electrophoresis (SDS-PAGE) was performed using 12.5% (w/v) gel, followed by transblotting to Immobilon-P transfer membranes (Millipore, Bedford, MA). Nonspecific bindings were blocked using Blockace solution (Dainippon Pharmaceutical Co., Osaka, Japan), and incubation with primary antibodies was carried out. After washing 3 times with tris-buffered saline with Tween 20, pH 8.0 (0.05 M Tris, 0.138 M NaCl, 0.0027 M KCl and 0.05% Tween 20; Sigma-Aldrich), the membrane was successively incubated with secondary antibodies and peroxidase activity was revealed using an ECL plus chemiluminescence kit (Amersham Pharmacia Biotech).

*Combination treatment with sequential addition of TRAIL and cisplatin*

KYSE cell lines sensitive to the combination treatments were cultured to subconfluence in 12-well tissue culture plates and 50 ng/ml TRAIL and 5 μg/ml cisplatin were added sequentially either TRAIL first, washed 3 times with PBS and then cisplatin, or *vice versa*, for 12 hr each. Crystal violet staining assays were then performed.

In vivo *treatments*

KYSE 170 cells ($5 \times 10^6$) were suspended in 100 μl PBS and inoculated subcutaneously into the right flank of the female nude mice, 5–6 weeks of age, of BALB/c background (Charles River Japan, Inc., Kanagawa, Japan). For the treatment of the established xenografts, the tumors were permitted to establish to the diameter of 6–7 mm for 10–14 days. Either cisplatin (1 mg/kg, 2 mg/kg, or 3 mg/kg), sterile normal saline (150 μl/body), or TRAIL (1 μg/body) was administered intraperitoneally (i.p.) daily for 4 consecutive days followed by 3 off-days per 1 course of a treatment. For the combination treatment, 2 mg/kg cisplatin and 1 μg/body-TRAIL were administered i.p. in the same dose schedule. Mice in all groups were treated for 2 consecutive weeks and then observed. Tumor growth was followed by measurements of tumor diameters with a sliding caliper 3 times a week, and mice were monitored daily. The tumor volume was calculated according to the following formula: $TV = L \times W^2/2$, where L and W are the major and minor dimensions, respectively. Systemic toxicity of the treatments was assessed by change in body weights. All treatment protocols were approved by the animal care and use committee of Kyoto University.

*Statistical analyses*

Commercially available software, Stat View version 4.5 (Berkeley, CA), was utilized for all statistical analyses. The correlations between various clinicopathological factors and sensitivity to the combination therapy were evaluated using Fisher's exact test and Kruskal-Wallis test. ANOVA Bonferroni test was used to evaluate the significance of differences in rates of apoptosis induction between combination therapies and single drug therapies. Mann-Whitney U-test was used to analyze the significance of difference of tumoricidal effects of the sequential treatment. In all tests, $p$ values less than 0.05 were considered significant.

## Results

*TRAIL receptor expression profiling in KYSE cell lines and PBMCs*

A summary of RT-PCR results on 19 KYSE cell lines and PBMCs is shown in Figure 1. DR4 and DR5 expression was detected in all of the cell lines; thus, they were ubiquitously expressed among KYSE cell lines. DcR1 was expressed in 18 of 19 cell lines (95%) and DcR2, in 15 of 19 cell lines (79%). There was only 1 cell line (KYSE 110) that was completely devoid of the decoy receptor transcripts. All 4 TRAIL receptor transcripts were detected in PBMCs.

*Tumoricidal effects of TRAIL and cisplatin against KYSE cell lines*

KYSE 110, 170 and 520 were subjected to the preliminary crystal violet staining assays. They had been selected because KYSE 110 is our only decoy-receptor negative cell line, and KYSE 170 and 520, which express all 4 TRAIL receptors, are 2 of the most frequently studied cell lines in our laboratory.[25,28] KYSE 110 and 170 were sensitive to the combination treatments, while KYSE 520 appeared to be resistant (Fig. 2*a*). Reduction of viable KYSE 110 and 170 cells by the treatment using 50 ng/ml TRAIL and 5 μg/ml cisplatin was statistically significant compared to either

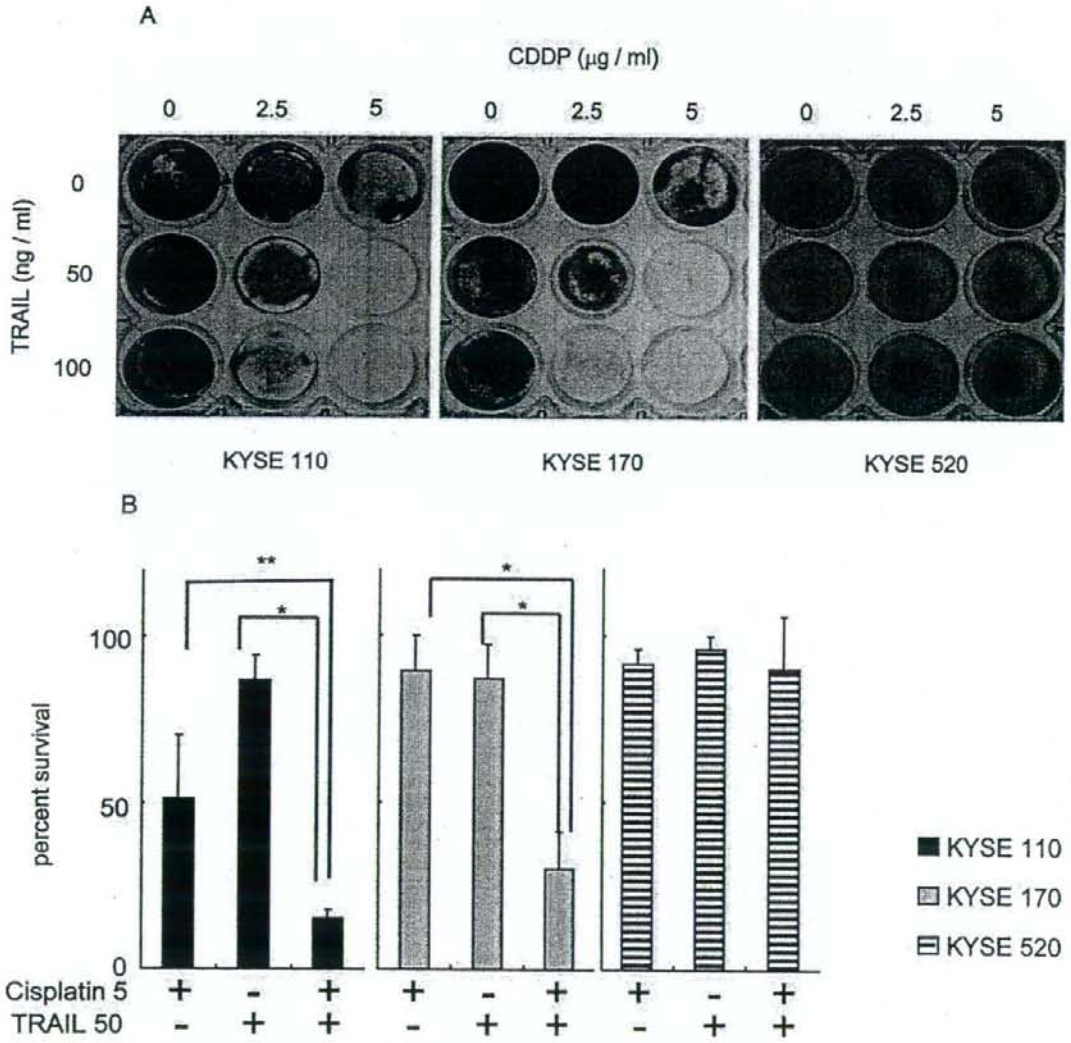


FIGURE 2 – (*a*) Crystal violet staining results after treatments with various concentrations of TRAIL and cisplatin for 24 hr are shown. KYSE 110 and KYSE 170 were sensitive to combination treatments, whereas KYSE 520 was resistant. Experiments were repeated 6 times per cell line, and the most representative results are shown. (*b*) Crystal violet staining results were quantified with OD absorbance. For each cell line, OD absorbance value for untreated control was arbitrarily set for 100%. All data are the mean of 4 independent experiments; bars represent SE. Cytotoxic effects in both KYSE 110 and KYSE 170 by the combination treatment was statistically significant compared to either single agent alone ($*p < 0.001$. $**p < 0.05$).

single agent alone, displaying synergistic effects (Fig. 2*b*). Hence, 50 ng/ml TRAIL and 5 μg/ml cisplatin were adapted to pursue further studies. Among 19 KYSE cell lines, KYSE 110, 170, 510, 850, 1190, 1860 and 2270 showed variable levels of sensitivity against the combination treatment and KYSE 2270 was the only cell line sensitive to TRAIL alone (Fig. 3). In the subsequent studies, KYSE 110 170, 1860 and 2270 had been selected because in these cell lines, viable cells were reduced significantly by the combination treatment, compared to either single agent alone. KYSE 960 and 1170 were used as resistant cell lines that lack DcR2 expression.

*Apoptosis induced by the combination treatment in KYSE cell lines*

To assess the type of cell death induced by TRAIL and cisplatin, flow cytometry was performed; Annexin-V binds to cells that express phosphatidylserine on the outer layer of the cell membrane, and PI stains the cellular DNA of cells with a compromised cell membrane. This allows for the discrimination of live cells (unstained) from early apoptotic cells (stained only with annexin-V) and late apoptotic or necrotic cells (stained with both annexin-V and PI). Cisplatin alone could induce a notable level of apoptosis only in KYSE 1860 (4.7% control *vs.* 30.8%) (Fig. 4*a*).

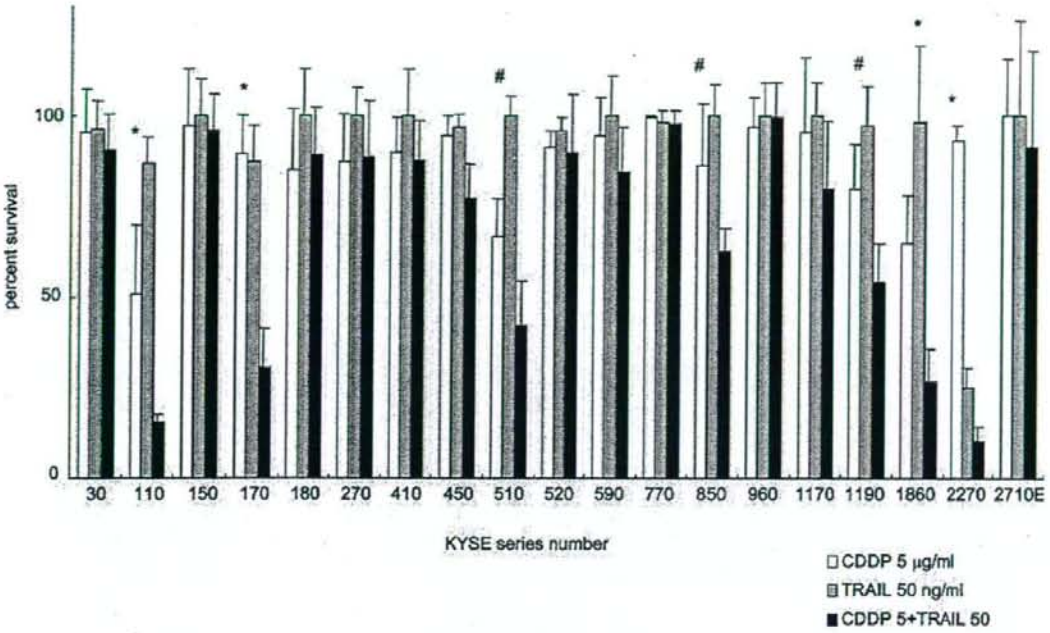


FIGURE 3 – After in contact with given doses of TRAIL and cisplatin for 24 hr, sensitivities of 19 KYSE cell lines to these agents either alone or in combination were evaluated with the crystal violet staining assays. Three cell lines (KYSE 110, 510 and 1860) and 1 cell line (KYSE 2270) showed some sensitivities to cisplatin and TRAIL, respectively. With the combination treatment, variable levels of cytotoxic effects were seen in 7 cell lines (KYSE 110, 170, 510, 850, 1190, 1860 and 2270). Asterisk indicates the cell lines in which cytotoxicity by the combination treatment was statistically significant ($p < 0.05$) compared to either single agent alone. Number sign denotes the cell lines in which cytotoxicity induced by the combination treatment was statistically significant compared to 1 of the 2 agents. Results indicate the mean of 4 independent experiments for each cell line.

TRAIL alone induced extensive apoptosis in KYSE 2270 (7.7% control *vs.* 88.5%) and some apoptosis in KYSE 170 (14.6% control *vs.* 35.3%) and 1860 (4.7% control vs. 21.9%). KYSE 110, despite absence of decoy receptors, did not undergo significant apoptosis when treated with TRAIL alone. However, the combination treatment resulted in synergistic cytotoxic effects. A majority of apoptotic cells in KYSE 110 was in early apoptosis while those in KYSE 170, 1860 and 2270 were in late apoptosis. By extending treatment periods to 48 hr, however, most of the apoptotic cells in KYSE 110 proceeded to a late apoptotic stage, revealing relatively slow progression of apoptotic process in KYSE 110 (data not shown). On the contrary, there was hardly any increase of apoptotic cells in KYSE 410, 520, 960 and 1170 (Fig. 4*b*), and these results were comparable with those in crystal violet assays. To further confirm that KYSE 170, 1860 and 2270 underwent apoptosis by the combination treatment, nuclear morphology was observed under fluorescent microscope, which revealed cells either in early or late apoptosis, but not in necrosis (Fig. 5). Meanwhile, PBMCs were resistant to both TRAIL and cisplatin, and the combination treatment could not induce apoptosis either (Fig. 4*b*).

*Demographic data analyses*

Clinicopathological data of 19 original ESCC are shown in Table I. Parameters compared are age and gender of the patients, TNM status, location of the primary tumor, TNM stage and histological grading of the resected tumor, against sensitivity to the combination treatment of TRAIL and cisplatin. In 1 of the patients, histological grading was not available. Although significant statistical differences could not be reached between cell lines sensitive to, and resistant to, the combination treatment in any of the criteria examined, well-differentiated SCC tended to be more resistant to the combination treatment, as 5 of 6 (83.3%) well-differentiated tumors were resistant, as opposed to 6 of 12 (50%) moderately and poorly differentiated tumors ($p = 0.316$).

*Activation of caspase cascade by the combination treatment*

TRAIL is known to induce apoptosis in target cells *via* activation of the caspase cascade (extrinsic pathway).[15,29] It has also been disclosed that caspase-8 can activate Bid of the Bcl-2 family to initiate the mitochondrial (intrinsic) pathway of apoptosis.[20,30,31] To unveil the TRAIL-mediated apoptosis pathway in KYSE cell lines, the expression of pro-apoptotic proteins caspase-8, -3, Bax, FADD and anti-apoptotic proteins Bcl-XL, FLIPL and XIAP has been investigated. First, in order to determine the optimal timing of protein extraction, KYSE 170 was treated with TRAIL and cisplatin, proteins extracted every 2 hr and activation of caspase-8 examined. An active form of caspase-8 was detectable within 4 hr and appeared to peak at 8 hr; hence, 8 hr contact time was deemed sufficient for protein extraction (Fig. 6). The baseline expression levels of these proteins in untreated controls are shown in Figure 7*a*. The expression levels of FADD, FLIPL and XIAP were variable among cell lines but there was no correlation between their expression levels and cell lines' sensitivity to the combination treatment. After the combination treatment, activation of caspase-8 and -3 was observed in KYSE 110, 170, 1860 and 2270 but not in KYSE 410, 520, 960 and 1170 (Fig. 7*b*). In order to elucidate intracellular changes involved in cisplatin-induced sensitization of esophageal SCC, Western blotting detection of FLIPS, FLIPL, XIAP and NFκB was further performed on both untreated cells and cells treated with 5 μg/ml cisplatin for

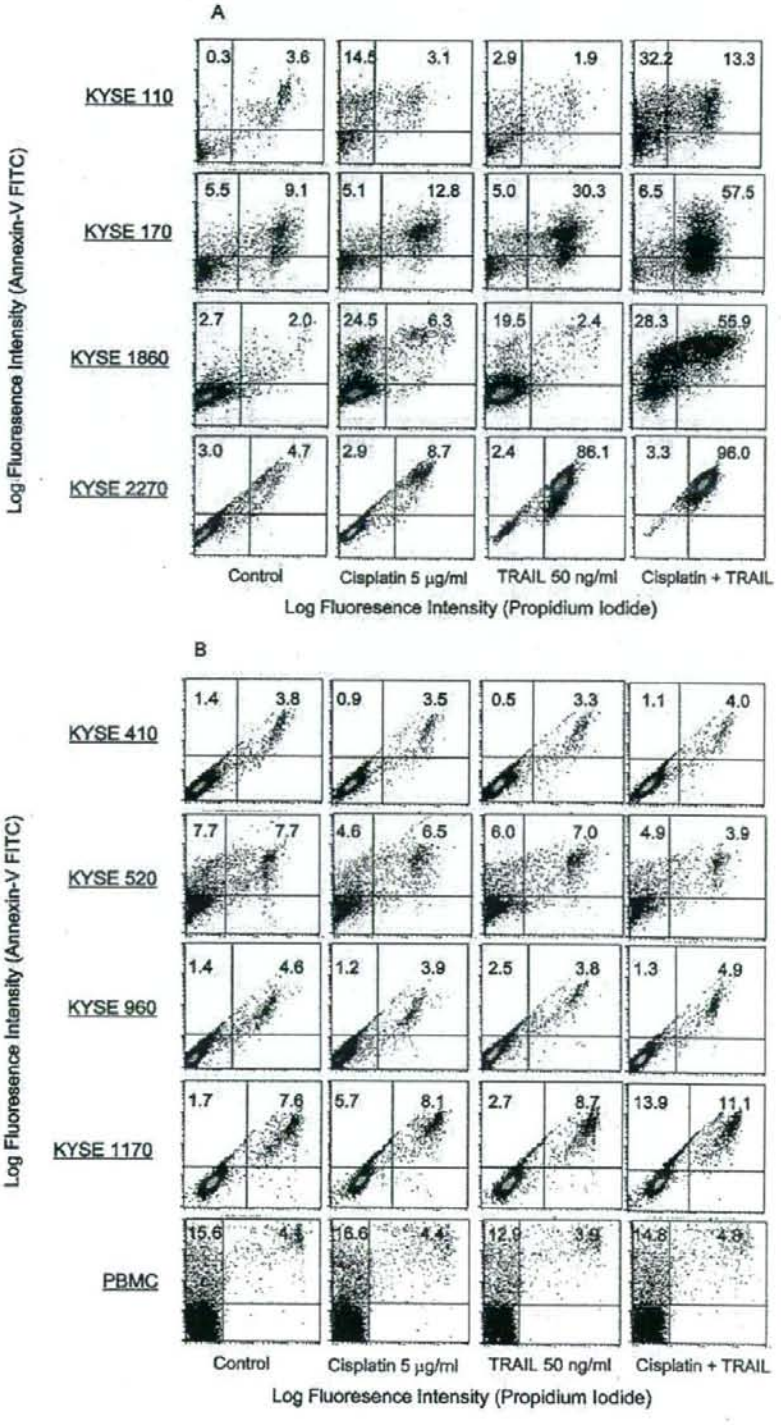


FIGURE 4 – Flow cytometric detection of apoptotic cells: Concentration of each agent used for "cisplatin + TRAIL" is 5 μg/ml and 50 ng/ml, respectively. Y-axis: Annexin-V conjugate. X-axis: Propidium Iodide uptake. Lower left quadrant, upper left quadrant, and upper right quadrant represent viable cells, cells in early apoptosis, and cells in late apoptosis respectively. Numbers in the diagrams show the percentage of cells represented in respective quadrants. (*a*) Cell lines sensitive to the combination treatment. Enhanced induction of apoptosis by the combination treatment was clearly observed in KYSE 110, 170, 1860 and 2270. B, KYSE 410, 520, 960, 1170 and PBMCs were resistant to the combination treatment and did not undergo apoptosis. Experiments were repeated at least 3 times for each cell line, and the most representative results are shown.

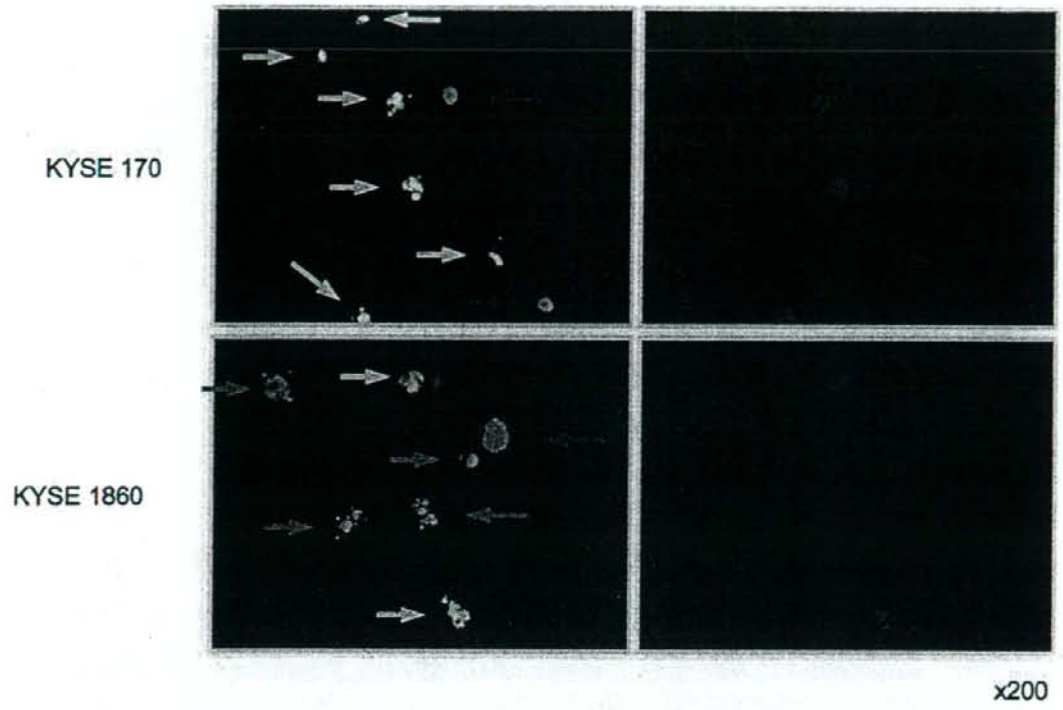


FIGURE 5 – Results of the morphological analyses of the nucleus using Hoechest 33342 and propidium iodide (PI) performed on KYSE 170 and 1860 after they had been treated with 50 ng/ml TRAIL and 5 μg/ml cisplatin for 24 hr. Left panels show Hoechest 33342 and PI staining. Right panels show the same view of the PI staining only. Most cells are either in early or late apoptosis, and necrotic cells were rather scarce. Intact blue nuclei (red arrow), condensed/fragmented blue nuclei (green arrow), condensed/fragmented pink nuclei (yellow arrow) and intact pink nuclei (not seen in the figure) represent viable, early apoptotic, late apoptotic and necrotic cells, respectively.

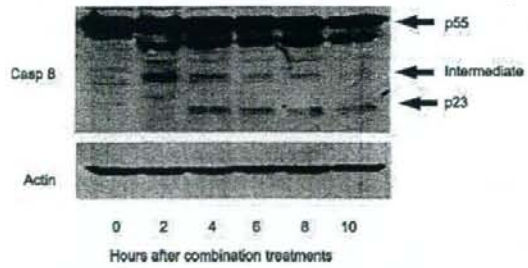


FIGURE 6 – Activation of procaspase-8 in KYSE 170. Cells were treated with TRAIL and cisplatin for indicated hours, and cell lysates were obtained for immunoblotting. An intermediate product of caspase-8 started to appear after 2 hr, and an active form was observable after 4 hr. Detection of the active form appeared to peak after 8 hr. Beta-actin expression is shown as a loading control. Experiments were repeated 3 times, and the most representative results are shown.

8 hr. Results are shown in Figure 7*c*. All 8 cell lines expressed FLIPL, FLIPS , XIAP and NFκB in various levels, and direct correlation between expression levels of these proteins and cell lines' sensitivity to the combination treatment was not apparent. However, slight decreases in expression levels of XIAP and FLIPS were noted in sensitive cell lines after the cisplatin treatment while their expression levels remained unchanged in the resistant cell lines. Meanwhile, expression levels of NFκB (p50, p65 and p115) and FLIPL remained unaffected by the cisplatin treatment (Fig. 7*c*).

*Cisplatin-induced upregulation of DR4 and DR5 in KYSE cell lines*

Influences of cisplatin on the surface expression of TRAIL receptors in KYSE cell lines were next investigated by flow cytometry, which clearly showed cisplatin-induced upregulation of both DR4/5 expression in KYSE 110, 170,1860 and 2270 after 6 hr exposure (Fig. 8*a*). On the other hand, their expression levels in KYSE 410, 520, 960 and 1170 remained nearly unchanged (Fig. 8*b*). Expression of the surface DcR1/2 paralleled that of mRNA transcripts but neither cisplatin-dependent upregulation nor downregulation was observed in any of the cell lines (Fig. 8*b*). Similar experiments were performed with PBMCs; DR4 was not detected on the surface of PBMCs even though DR4 mRNA was present by RT-PCR. DR5, DcR1 and DcR2 were detectable, but their expression levels were not influenced by the exposure to cisplatin.

*Sensitization of KYSE cell lines to TRAIL by pretreatment with cisplatin*

From the results thus far, upregulation of DR4/5 by cisplatin may be a critical factor rendering cells sensitive to the combination treatment. To confirm this, crystal violet staining studies were carried out in sensitive cell lines by sequentially adding cisplatin and TRAIL. Since KYSE 2270 was sensitive to TRAIL, signifi-